# Nanocelllulose Based Adsorbents for Heavy Metal Ions Removal

**Rongrong Si**
Qilu University of Technology
**Daiqi Wang**
Qilu University of Technology
**Yehong Chen**
Qilu University of Technology
**Dongmei Yu**
Qilu University of Technology
**Qijun Ding**
Qilu University of Technology
**Ronggang Li**
Qilu University of Technology
**chaojun wu** ( chaojunwu2007@163.com )
Qilu University of Technology https://orcid.org/0000-0002-7840-0077

**Research Article**

**Keywords:** nanocellulose, modification, heavy metal ions, assembling, adsorbent

**Posted Date:** June 15th, 2021

**DOI:** https://doi.org/10.21203/rs.3.rs-594942/v1

# Abstract

Heavy metal ion pollutions are of serious threat for our human health, and advanced technologies on removal of heavy metal ions in water or soil are in the focus of intensive research worldwide. Nanocellulose based adsorbents are emerging as an environmentally friendly appealing materials platform for heavy metal ions removal as nanocellulose has higher specific surface area, excellent mechanical properties and good biocompatibility. In this review, we briefly compare the differences of three kinds of nanocellulose and their preparation method. Then we cover the most recent work on nanocellulose based adsorbents for heavy metal ions removal, and present an in-depth discussion of the modification technologies for nanocellulose in assembling high performance heavy ions adsorbent process. By introducing functional groups, such as amino, carboxyl, phenolic hydroxyl, and thiol, the nanocellulose based adsorbents not only remove single heavy metal ions through ion exchange, chelation/complexation/coordination, electrostatic attraction, hydrophobic actions, binding affinity and redox reactions, but also can selectively adsorb multiple heavy ions in water. Finally, some challenges of nanocellulose based adsorbents for heavy metal ions are also prospected. We anticipate that the review supplies some guides for nanocellulose based adsorbents applied in heavy metal ions removal field.


# 1. Introduction

Nowadays, heavy metal ions has become the most serious problem in water environment due to their toxicity and incompatibility, which not only cause badly problems of environmental but also threaten health of human(Miretzky and Cirelli 2009). Excessive intake of heavy metal ions can cause body damage and even death, such as, Minamata(Petrova et al. 2020) disease in Japan caused by the excessive intake of organic mercury (Hg),some lungs or gastrointestinal tract disease caused by the accumulation of $Cd^{2+}$(Anetor 2012), and Alzheimer's and Parkinson's diseases(Du et al. 2018) caused by the excessive intake of $Fe^{3+}$and $Al^{3+}$.In addition, the rise of nuclear power plants will also cause many radioactive heavy metal pollution such as ($Cs^{137}$, $Pu^{239}$ and $U^{238}$)(Buesseler et al. 2012).It is challenging to attenuate or eliminate heavy metal ion pollutions.

There are many methods to solve heavy metal ions pollution problems in wastewater, mainly include chemical precipitation, ions exchange, ultrafiltration, flocculation, electrodialysis, adsorption and reverse osmosis, etc.(Fu and Wang 2011) Among these methods, adsorption is the most widely used one due to the high removal efficiencies, flexibility in the design and low cost(Shen et al. 2019). The adsorbents mainly include activated carbon, clay, biochar and polymers(Qin et al. 2019b). Recently, nanocellulose-based adsorbents become more and more popular as nanocellulose has higher specific surface area, excellent mechanical properties and good biocompatibility(Jordan et al. 2019).

In this review, we first summarize categories, characteristics and preparation methods of nanocellulose. Then, we present the most recent work on nanocellulose based adsorbents, and deeply highlight the roles of nanocellulose in nanocellulose based adsorbents. Finally, we conclude with perspectives on the remaining challenges and potential opportunities of nanocellulose based adsorbents.

# 2. Classifications Of Nanocellulose

Cellulose is photosynthesized from $CO_2$ and water, and accumulated as a major component in plants(Isogai 2020). It is a crystalline biopolymer possessing long chains of β-D-glucopyranose units joined by β-1,4 glycosidic linkage in which inter- and intramolecular hydrogen bonding restrict its main chain motion(Garba et al. 2020). It is evident that the adsorption properties of native cellulose can be increased by converting it to the nanostructure(Kardam et al. 2014). According to the work of Vadakkekara(Vadakkekara et al. 2019) et al. the maximum adsorption capacity (115 mg/g) of maleic acid-modified nanocellulose for $Pb^{2+}$ is higher than that of maleic acid-modified macro(20mg/g) or micro cellulose(40mg/g).

Nanocellulose (NC) is a cellulose material with at least one dimension in the nanometer size range separated from fiber raw materials through physical, chemical or biological treatment(Li et al. 2010). Depending on its cellulose source, processing conditions, size, function and preparation methods, it can be classified into three categories such as nanofibrillated celluloses (NFCs), bacterial nanocellulose (BNCs) and cellulose nanocrystals (CNCs). CNCs, also known as nanowhiskers, exhibit elongated crystalline rod-like shapes, and have high rigidity compared to NFCs since their amorphous regions are highly removed. Nanofibrillar cellulose, cellulose nanofibers, and cellulose nanofibrils are some of synonyms for NFCs(Li et al. 2017), and their cellulose chains are entangled and flexible with a large surface area. BNCs are fairly straight and continuous and have low polydispersity in terms of their dimensions. Scanning electron microscope (SEM) images of three types of nanocellulose are showed in Fig. 1a (NFCs(Wang et al. 2020a)), b(CNCs(Li et al. 2019b)) and c(BNCs(Zhu et al. 2011)).

To obtain different structures and properties of NFCs, some researchers usually use mechanical treatments, mainly including high-pressure homogenization, grinding, micro-jetting, freezing crushing, and high-intensity ultrasound(b et al. 2014), and combined with pretreatment technologies, such as, organic acid hydrolysis(Du et al. 2016), periodate oxidation(Larsson et al. 2014), TEMPO(2,2,6,6-Tetramethyl-1-piperidinyloxy)(Saito et al. 2007) oxidation, eutectic solution(Liu et al. 2019), ionic liquid(Ninomiya et al. 2018) etc. to prepared NFCs from cellulose raw materials. The preparing methods of CNCs mainly include acid hydrolysis and enzymatic(Tong et al. 2020) hydrolysis. Acid hydrolysis usually uses strong inorganic acids(Naduparambath et al. 2018; Yani et al. 2017) (such as sulfuric acid, hydrochloric acid, etc.) to hydrolyze the amorphous regions in the cellulose structure to separate cellulose crystals. In order to obtain the desired structures and properties of CNCs, some environmental friendly pretreatments also have been gradually applied in the preparing processes of CNCs, such as organic acid hydrolysis(Chen et al. 2016), solid acid hydrolysis(Liu et al. 2014b), eutectic solvent(Gan et al. 2020) etc. BNCs are produced by cultivating bacteria(*Gluconoacetobacter xylinus family*, Agrobacterium, Pseudomonas, Rhizobium, and Sarcina (El-Saied et al. 2004)) for a few days in an aqueous culture media containing glucose, phosphate, carbon, and nitrogen sources. To obtain the desired structures and properties of BNCs, we can realize by regulating the nutrient source, oxygen ratio, bacterial strain type, incubation time, and cultivation in a bioreactor(Tang et al. 2017).

To date, the three kinds of nanocelluloses are not only were used in conductive materials, oil-water separation, filter materials, food processing, sensor, capacitor, bio scaffold, and drug delivery fields, but also applied in the fields of heavy metal ions removal and become more and more popular.

# 3. Nanocellulose Based Adsorbents For Single Heavy Ion Removal

## 3.1 Nanocellulose based adsorbents for $Cu^{2+}$ removal

Generally, natural nanocellulose is challenged by intrinsic hydrophilicity and inferior adsorption sites, which thus affect its performance in extraction of heavy metal ions(He et al. 2018). However, the high number of hydroxyl groups on the surface of cellulose fibers can provide a platform to modify it with different properties. Qin et al. (2019a) treated different amounts of wood fibers with monochloroacetic acid/sodium hydroxide and homogenization to obtain carboxymethylation CNF(CMCNFs) with different carboxyl content. CMCNFs showed diameters of 3.40 − 3.53 nm and lengths of 1210.6 − 383.3 nm. The carboxyl group content of CMCNF can reach up to 2.7mmol/g(CMCNF-2.7), and the maximum zeta potential value is -88.3mV. Since the carboxylate group of CMCNF can capture $Cu^{2+}$ through electrostatic attraction, ion exchange and complexation actions, its maximum adsorption capacity for $Cu^{2+}$ reaches 115.3mg/g at pH 5.

By controlling different degrees of Tempo oxidation, Liu et al.(2016) obtained two kinds of TOCNFs from Cellulose sludge with different carboxyl content (0.6, 1.5mmol/g). The adsorption mechanism and properties of $Cu^{2+}$ were investigated. $Cu^{2+}$ can be adsorbed on the surface by carboxyl groups, and then reduced to copper (0) or assembled copper oxide nanoparticles by micro precipitation. Copper adsorption increased with the enhancement of copper concentration up to 44.2 mg/g and 75 mg/g for TOCNF0.6 and TOCNF1.5.

Fan et al.(2019) obtained CNCs (CNCs-2h, 4h, 6h, 8h) with different carboxyl content through $Fe^{2+}/H_2O_2$ oxidation of MCC for different durations (2,4,6,8 h). CNCs with a size of 92-140nm in length and 19-23nm in width. The results indicated that the CNCs-6h with the highest carboxyl content (2.2mmol/g) and the maximum zeta potential value is -41mV. Because the carboxylic acid groups in Carboxylated CNCs have a significant capability to bind $Cu^{2+}$, the maximum adsorption capacity is 51.1mg/g.

Tang et al. (2020a) firstly disperse CNF slurry with different concentrations in liquid nitrogen and rapidly freeze to form spherical beads and freeze-dry to obtain CNF cryogel beads. Then the carboxylated CNF/maleic anhydride cryogel beads (CNF-MA) was obtained by mixing and reacting the original CNF cryogel beads and maleic anhydride (MA) solution. Its carboxyl content reaches 2.78mmol/g and maximum adsorption capacity for $Cu^{2+}$ reaches 82.17mg/g. Desorption experiments with EDTA-$Na_2$ showed that its adsorption capacity for $Cu^{2+}$decreased from 68mg/g to 45mg/g after 4 cycles.

Wang et al. (2018a) obtained 9-CNF, 7-CNF and 5-CNF with different carboxyl contents according to different ratios of hydrochloric acid/ citric acid (v/v = 9/1, 7/3, 5/5) waste ginger fiber. As a comparison,

S-CNF was obtained by traditional sulfuric acid hydrolysis. Hereafter, CNF suspension freeze-dried to obtain aerogels. 3D network structures of all aerogels were physically cross-linked by hydrogen bonding with mesopores to macropores (Fig. 2). Among them, 7-CNF had the largest aspect ratio (144) and the largest carboxyl content (1.18 ± 0.1mmol/g) and largest negative zeta potential (-36 ± 3mV). Compressive properties (99.5kPa at 80% strain, 241.77 kPa at 90% strain) at a low density of 20.3 mg/cm$^3$. Its maximum adsorption capacity for $Cu^{2+}$reached 45.053mg/g due to the network capture effect, charge neutralization and chain bridging of high aspect ratio carboxylated CNF.

Lei et al. (2019) obtained NFCs suspension after grinding through *Endoglucanase* enzymolysis, adjusted the concentration of sodium periodate to 10 (DNFC-1), 40g/L (DNFC-2) to controlled the content of aldehyde group. DNFC-2 has the largest aldehyde content (1.95 mmol/g), biggest specific surface area (2.73 ± 0.08m$^2$/g), and the surface charge density of (1.14 ± 0.07) ×10$^{-5}$eq/g. The maximum adsorption capacity of DNFC-2 for $Cu^{2+}$ was 26mg/g.

Ji et al. (2020) used a simple co-deposition coating process to cover tannic acid (TA) and different amounts of cardanol-derived siloxane (CDA) onto the CNF framework, and then freeze-dried to obtain a porous structure TA@CNF-CDA aerogel. Since TA contains many pyrogallol functional groups and has excellent chemical reactivity with thiol or amine terminal monomers(Wang et al. 2018d), so it can provide an active intermediate layer to improve adsorption efficiency for $Cu^{2+}$. The contact angle and Brunner – Emmet – Teller (BET) surface area of the aerogel are 121° and 75.66m$^2$/g, respectively. Its maximum adsorption capacity for $Cu^{2+}$reaches 45.6mg/L due to the higher catechol groups on the surface of the aerogel.

Amino groups have a strong chelating ability to heavy metal ions, so increasing the amino group content can increase the adsorption capacity. Since polyethyleneimine (PEI) has plenty of primary, secondary and tertiary amines on the macromolecular chains, it was usually fabricated hydrogels or aerogels by crosslinking with an aldehyde or epoxy group for improving the adsorption capacity(Shao et al. 2017). Tang et al. (2020b) obtained a high amine group content(5.74mmol/g) of cellulose nanofibril/PEI aerogel bead (CGP1.3) with the help of a cross-linking agent of 3-glycidyloxypropyl) trimethoxy silane (GPTMS) by quickly frozen with liquid nitrogen and freeze-dried methods. Its maximum $Cu^{2+}$ adsorption capacity reached163.40mg/g. Mo et al. (2019) used TO-CNF and Trimethylolpropane-tris-(2-methyl-1-aziridine) propionate (TMPTAP) to react through a ring-opening reaction at room temperature, and post-crosslinked PEI to obtain a 3D multi-wall structure TO-CNF/TMPTAP/PEI aerogel (TO-CTP)with pores. Since the aerogel had a large number of amino groups and oxygen-containing groups on the surface, its maximum adsorption capacity for $Cu^{2+}$reached 485.44mg/g. Moreover, after being treated with EDTA-2Na, the regenerated aerogels also retained high removal efficiency for $Cu^{2+}$ over four desorption-regeneration cycles.

Zhang et al.(2016) obtained TOCN by HCl hydrolysis and TEMPO oxidation, and then cross-linked with PEI under the action of glutaraldehyde (GA) cross-linking agent, then freeze-dried and grinded to get

TOCN-PEI adsorbent. Because of the linking between PEI and -COOH, the carboxyl content of TOCN-PEI decreased from 1.88 to 0.85 mmol/g, and its total amount of amino groups was 4.06 mmol/g. Its maximum capacities for $Cu^{2+}$ reached 52.32mg/g due to its abundant carboxyl and amino groups. After HCl cleaning, its adsorption capacity could still reach 33mg/g.

Tang et al.(2020c) controlled different $H_2O_2$ oxidation time (3h, 6h, 9h), and oxidized pomelo peel to obtain anionic/carboxyl nanocellulose (POCNF-3, 6, 9), the obtained POCNF-6 had the highest carboxyl group content (1.711 ± 0.173mmol/g), highest aspect ratio (169) and largest negative zeta potential(30.5 ± 2.7). Hereafter, POCNF-6 crosslinked with PEI under the action of a glutaraldehyde crosslinking agent to obtain POCNF-PEI. Its maximum adsorption capacity for $Cu^{2+}$ reached 74.2mg/g. The $Cu^{2+}$ adsorption capacity of POCNF-PEI remained to 66.2 mg/g after four adsorption-desorption cycles.

The composite of two or more polymers has become a new development trend of biomaterials in order to obtain certain excellent properties that a single polymer cannot achieve(Cui et al. 2015). Polydopamine (PDA), formed by self-polymerization of dopamine, is rich in catechol and amine groups, which facilitate covalent conjugation or other noncovalent interactions with organic and inorganic materials(Liu et al. 2011). Juntao et al.(2019) used a bio-inspires coating strategy to introduce PDA particles into the surface of CNFs, and then cross-linked PEI to form porous aerogel (PDA-CNF-PEI). Its maximum adsorption capacity for $Cu^{2+}$ reached 103.5mg/g, and its porosity and density were 98.5% and 25mg/$cm^3$, respectively. When it was regenerated for four cycles by using 0.1M HCl treatment, its adsorption efficiency for $Cu^{2+}$still retained more than 91%.

Mautner et al.(2016) modified the cellulose nanofibrils from the fiber sludge with phosphoric acid to obtain phosphorylated cellulose nanofibrils, and then prepared nanopapers(CNF-P) through papermaking methods. Its maximum adsorption capacity for $Cu^{2+}$ could reach 19.6mg/g by the ion exchange capture action of phosphate groups in CNF-P (18.6 ± 2.3mmol/kg). After a simple washing of phosphoric acid, the adsorption capacity of $Cu^{2+}$ can still reach 19.4mg/g.

# 3.2 Nanocellulose based adsorbents for $Pb^{2+}$ removal

Francisco et al.(2020) obtained cellulose from raw agave leaves by benzyl alcohol extraction, sodium hydroxide alkali treatment and peracetic acid (PAA, $H_2O_2$ + acetic acid + $H_2SO_4$), and then high-pressure treatment with a microfluidization process to obtain cellulose nanofibrils and nanosheet (CNF/CNS). The results showed that the CNF/CNS surface contained a lot of carboxyl groups. At low initial concentrations of $Pb^{2+}$ (C0 < 100 ppm), the adsorption-mechanism is governed by electrostatic interactions between carboxylate groups and $Pb^{2+}$; meanwhile, at (C0 = 1000 ppm) mono and bi-dentate complexes dominate the adsorption-mechanism. Finally, when 110 < C0 < 1000 ppm, both mechanisms co-exist. According to Langmuir model, the maximum adsorption capacity for $Pb^{2+}$ was 43.55mg/g.

Sharma et al. (2018b) used nitric acid/sodium nitrite to oxidize untreated jute fibers to obtain NOCNF slurry. Although its crystallinity was very low (35%), its carboxyl content and surface charge were very

high (1.15mmol/g and − 70mV). At a low NOCNF suspension concentration (0.23wt%), room temperature, pH = 7, the NOCNF could remove sharply $Pb^{2+}$ ions of from 50 to 5000ppm in the initial steps, and finally its maximum adsorption capacity could reach 2270mg/g.

Graphene oxide (GO) was used to remove heavy metal ions due to its high specific surface area and large number of functional oxygen groups that could provide active sites for heavy metal ions(İlayda et al. 2016). Yu et al. (2020) used $Fe^{3+}$ as crosslinking agent, carboxymethyl cellulose nanofibril as filler, and wet-spinning method to obtain GO/CMCNF composite fiber(CF). The fiber exhibited enhanced mechanical property up to 648MPa. Its maximum adsorption capacity for $Pb^{2+}$ reached 99.0mg/g by electrostatic attraction, ion exchange and complexation of carboxyl groups and $Pb^{2+}$.

Alginate could be also mixed with nanocellulose to remove heavy ions in water due to its non-toxic, biodegradable, low cost and rich carboxyl groups(Eldin et al. 2016). Hu et al.(2018) cross-linked carboxylated cellulose nanocrystal(CCN) and sodium alginate under the action of $Ca^{2+}$ to obtain CCN-Alg hydrogel. It was easy to separate after adsorption, and had stronger mechanical strength and durability than pure sodium alginate beads. The proposed adsorption mechanisms could possibly include electrostatic attraction and complexation. Within two hours, 76% of $Pb^{2+}$ could be removed, and adsorption equilibrium was quickly reached in three hours, and the highest adsorption capacity was 338.98mg/g.

Activated carbon (AC) is widely used in the removal of heavy metal ions due to its high specific surface area and fast adsorption speed(Lee et al. 2021). Sari et al. (2017) successfully extracted AC from recovered PACl-lignans containing black liquor sludge. In another work, Septevani et al.(2020) used sulfuric acid or phosphoric acid to hydrolyze *oil palm empty fruit bunches* to obtain nanocellulose (NCS, NCP). Then use the obtained AC to activate NCS/NCP. The SEM image showed that AC was dispersed in the NC matrix, forming a looser embedded network. Its adsorption mechanism was mainly the electrostatic attraction between adjacent hydroxyl groups and positively charged metal ions on the surface of the super-adsorbent, and its maximum adsorption capacity for $Pb^{2+}$ reached 24.94mg/g.

In order to improve the hydrophobicity and flexibility of nanocellulose based adsorbents, Rani et al.(2019) used steam explosion method to extract CNCs from banana fiber, and grafted butyl acrylate(BA) onto CNCs to obtain CNCs-g-nBA membrane with the help of ceric ammonium nitrate initiator. Its adsorption capacity changed with the different pH values of the solution. At low pH, the concentration of protons in the solution was high, and the metal binding site became positively charged, repelling $Pb^{2+}$ cations. As the pH raised, the negative charge density on the adsorbent increased due to the deprotonation of the metal binding site, and adsorption capacity enhanced, however, at pH > 6, the formation of aqueous metal hydroxide precipitation was the main mechanism for removal. At pH = 5, its maximum adsorption capacity with $Pb^{2+}$ reached 159.53mg/g, and after 3 cycles of desorption with 0.1N HCl and 0.1M EDTA, its adsorption capacity could still maintain a high potential.

Polyvinyl alcohol (PVA) is an inexpensive polymer which possesses desirable properties such as water solubility, biocompatibility, and biodegradability. The application of magnetic adsorbents technology has become one of the promising ways to solve environmental problems(Feng et al. 2010). Zhou et al.(2013) used TEMPO to oxidize MCC to firstly obtain carboxylated cellulose nanofibrils (CCNFs) and then obtain CCNFs-filled magnetic chitosan hydrogel beads (m-CS/PVA/CCNFs) through an instantaneous gelation method. It had a 3D porous structure (Fig. 3(a)), m-CS/PVA/CCNFs hydrogel beads can be easily separated from water (Fig. 3(b)). Its removals for $Pb^{2+}$ were mainly through amino chelation and carboxyl ion exchange. Its maximum adsorption capacity for $Pb^{2+}$ could reach 171.0mg/g. After four cycles with weak acid regeneration, its adsorption efficiency could still retain 90%.

Vadakkekara et al. (2020) obtained nanocellulose from *jute fiber*, and then modified it with sodium itaconate to obtain sodium itaconate grafted nanocellulose(SINC) adsorbent. The SEM image showed that the SINC surface was irregularity and smoothness. Its maximum adsorption capacity for $Pb^{2+}$ was 85mg/g at the pH value of 5.5.

# 3.3 Nanocellulose based adsorbents for $Cr^{6+}$ removal

Cr is one of priority pollutants in water. Cr has two common oxidation states, $Cr^{6+}$ is highly toxic, mutagenic and carcinogenic to the ecosystem, however, $Cr^{3+}$ is a nontoxic substance(Wang et al. 2015).

For the removal of hexavalent chromium ($Cr^{6+}$) ions(Attia et al. 2010), most adsorbents have a higher efficiency when pH value was less than 3, but under neutral or alkaline conditions, the removal efficiency was relatively lower. Huang et al. (2020) oxidized *sugarcane bagasse* with sodium periodate and followed by cationization using Girard's reagent T to obtain cationic dialdehyde cellulose (c-DAC). There were high density of quaternary ammonium groups and aldehyde groups on the surface of c-DAC. The electrostatic attraction between the positively charged quaternary ammonium salt group and the negatively charged dichromate was the main mechanism of adsorption, and there was a strong binding affinity between the adsorbent and $Cr^{6+}$. When the adsorption reached saturation, the surface charge on c-DAC was neutralized to form c-DAC-chromium flocs, which could easily be removed by decantation or low-cost gravity-driven microfiltration. The maximum adsorption capacity for $Cr^{6+}$ could reach 80.5mg/g, and it had stable adsorption performance under a wide pH range (2–10).

Ferreira-Neto et al.(2020) prepared a self-supported hybrid aerogel film(BC/$MoS_2$) combining Bacterial nanocellulose-based organic macro/mesoporous scaffolds and $MoS_2$ nanostructures(Fig. 4). Since $MoS_2$ is a transition metal hydrogen disulfide, a layered structure composed of stacked two-dimensional nanosheets(Wang et al. 2018c), this film displays a large number of sulfide($S^{2-}$) sites, which was easy to bind heavy metal ions by electrostatic or hydrophobic adsorptions. Its specific surface area and pore volume were 97-137$m^2$/g and 0.28-0.36$cm^3$/g, respectively. $Cr^{6+}$ is removed through adsorptive-photocatalytic mechanism since $MoS_2$ showed effective visible light photoactivity (Fig. 4(b)). Remove $Cr^{6+}$ ion (88% removal within 120min, Kobs = 0.0012$min^{-1}$) in photos assisted in-flow.

Zhao et al.(2015) used bamboo pulp to perform ultrasonic and high shear homogenization to obtain CNFs ((Fig. 5 (a, b)). Then, the CNFs were modified with amino groups by Michael reaction, and finally the terminal ester groups were amidated with ethylenediamine (EDA). Repeated several times to obtain PAMAM-g-CNFs, and freeze-dried to obtain PAMAM-g-CNFs aerogel (Fig. 5 (c)). Poly(amidoamine) (PAMAM)(Han et al. 2012) contains a large number of amine groups and amide groups and is common dendrimers. The aerogel has a porosity of 99.39%, specific surface aera is 82$m^2$/g and a density of 0.01g/$cm^3$. The aerogel removes $Cr^{6+}$ through ion exchange and redox reactions. First, the amino group is protonated under acidic conditions, and $Cr^{6+}$ is electrostatically attracted to the aerogel on the surface, part of $Cr^{6+}$ is reduced to $Cr^{3+}$ by the adjacent electron donor groups. The positively charged $Cr^{3+}$ is released in the water. Some $Cr^{3+}$ ions can still form stable complexes with the negatively charged groups of PAMAM-g-CNFs (Fig. 5(d)). These led to its maximum adsorption capacity of 377.36mg/g for $Cr^{6+}$.

Ram et al. (2018) obtained spherical nanocellulose(SNC) through acid hydrolysis, then oxidized it with sodium periodate, and further processed it with 2-aminoethane-1-sulfonic acid to obtain Schiff base. Finally, a SNC-Chemosensor was obtained after adding mercaptopropionic acid (MPA) and a specific amount of lipase. Its adsorption mechanism mainly was the complexation of imine, sulfonate and thioester functional groups with $Cr^{6+}$, furthermore, the phenomenon of charge transfer from the ligand to the metal also led to the naked eye color sensing in the range of 30ppb to 100ppm of $Cr^{6+}$. Its maximum adsorption capacity for $Cr^{6+}$was 130mg/5mg at pH = 7 and could be easily regenerated with 0.1M NaOH since it contained imine, thioester and sulphonate groups.

Shahnaz et al. (2020a) hydrolysis cellulose with sulfuric acid to obtain spherical NC and coupled with polypyrrole (PPY) to obtain an adsorbent (NCPPY) for $Cr^{6+}$ removal in water. Since polypyrrole (Lei et al. 2012) is an organic polymer formed by polymerization of pyrrole ring ($C_4H_5N$), extensive studies on this polymer justifies its stability, low cost and eco-friendly nature. Compared with 197$m^2$/g for NC, the specific surface area of NCPY was significantly increased (488$m^2$/g). The maximum adsorption capacity of NCPPY for $Cr^{6+}$ was 147.3mg/g possibly duo to the -OH and -$NH_2$ adsorption sites on its surface.

# 3.4 Nanocellulose based adsorbents for $Hg^{2+}$ removal

Silva et al. (2020). dissolved lysozyme protein extracted from egg white in a solution containing 20 mmol/L glutamic acid and 5% (V/V) DES (choline chloride/acetic acid) to obtain lysozyme nanofibrils (LNFs)(Silva et al. 2018),and then mixed with different proportions of CNFs to obtain dual-nanofibrillar films (CNFs/LNFs). Combined the advantages of CNFs with high specific surface area and LNFs with a large number of peptide R-groups on their surface, the films had a strong mechanical properties and binding capacity for $Hg^{2+}$. The removal efficiency is pH-dependent reaching a maximum of 99 % (50μg/L) after 24 h at a pH value close to the isoelectric point of the protein.

It was reported that thiol groups had highly selective adsorption of $Hg^{2+}$ from wastewater(Yantasee et al. 2007). Geng et al.(2017) oxidized bamboo-derived cellulose with TEMPO to obtain TO-NFC, and then

subjected to facile freeze-drying in MPTs(3-mercaptopropyltrimethoxysilane) sols to obtain flexible aerogel(TO-NFC-Si-SH). The aerogel had a high SH content of 3.33mmol/g, and its porosity reached 99.1%, the BET specific surface area was 43.57$m^2$/g, and the removal rate could reach more than 92% in the $Hg^{2+}$ solution at range of 0.01-85mg/g. According to the hard – soft acid base (HSAB)(Wang et al. 2020b) theory, $Hg^{2+}$ ions are classified as a Lewis soft acid, while thiol and carboxylate groups belong to Lewis soft and hard bases, respectively. Therefore, thiol groups on TO-NFC-Si-SH aerogel tended to be preferentially complexed with $Hg^{2+}$ compared with carboxyl groups. Its maximum adsorption capacity for $Hg^{2+}$ reached 718.5mg/g. Moreover, its adsorption capacity was nearly unchanged at a large pH range. After four adsorption/desorption experiments with 0.1M HCl/5wt% thiourea, its adsorption efficiency could still retain more than 90%.

Rong et al. (2018) used TEMPO to oxidize wood pulp to obtain CNF, and 3-mercaptopropyltrimethoxysilane (MPTMS) (MPTMS: CNF = 1/2) was added to the CNF suspension at room temperature to obtain CNF-1MPTMS and CNF-2MPTMA, then quickly frozen in liquid nitrogen and vacuum dried for 24 hours to obtain CNF-MPTMS sponge. There is a porous structure on the surface, the specific surface area and porosity of CNF, CNF-1MPTMS and CNF-2MPTMA are 12.99, 10.94, 8.84$m^2$/g and 89, 93, 95% respectively (Fig. 6). The maximum adsorption capacity of CNF-2MPTMA for $Hg^{2+}$ could reach 700mg/g. After using 0.1M aqueous disodium edetate dihydrate solution to remove $Hg^{2+}$, the adsorption capacity of CNF-MPTMS sponges did not decrease significantly.

Chauhan (2018) obtained spherical nanocellulose (SNC) by the treating sequences with NaOH and mixed acid of sulfuric acid/hydrochloric acid and ultrasonication, and then enzymatically esterified SNC with 3-mercaptopropionic acid (3-MPA) to obtain its ester derivative (SNC- 3-MPA). $^{13}$C-NMR (nuclear magnetic resonance) results showed that the thiol group was grafted onto C-6-0 of cellulose monomer rings. Since SNC has a higher specific surface area than cellulose and the presence of thiol groups had a high affinity for $Hg^{2+}$, so the removal rate of $Hg^{2+}$ at a concentration of 100 ppm could be as high as 98.6% within 20 minutes. It can be recycled with 0.1N HCl. The adsorbent can be regenerated and its reusability was studied up to nine cycles with cumulative adsorption capacity of 404.95 mg/g.

In order to use the two functional groups(thiol and amino groups) in its molecular structure, Li et al. (2019b) hydrolyzed the qualitative filter paper with sulfuric acid, followed by mechanical treatment to obtain CNC, oxidized the CNC with sodium periodate to obtain with different aldehyde group content dialdehyde cellulose nanocrystals ($DAC_{1.84, 2.25, 4.05}$). After modification of three DAC with cysteamine, Cys-$CNC_{1.84, 2.25, 4.05}$ were obtained. There was a strong binding interaction between thiol group and $Hg^{2+}$ of Cys-CNCS. The maximum adsorption capacity of Cys-$CNC_{4.05}$ for $Hg^{2+}$ is 849mg/g. In a 51mg/L $Hg^{2+}$ solution, Cys-$CNC_{4.05}$ can remove 99% within ten minutes. 2M HCl and 0.5M thiourea as the eluent were used to regenerate Cys-CNCs. The removal percentage of $Hg^{2+}$ for Cys-$CNC_{4.05}$ still remained 90% after four adsorption – desorption cycles.

# 3.5 Nanocellulose based adsorbents for radioactive heavy ions

At present, nuclear energy accounts for 14% of the total energy system and generates approximately 200 ~ 300 tons of nuclear waste every year. These radioactive nuclear wastes have harmful effects on animals and plants in the ecosystem, causing pollution to the environment(Park et al. 2020).

Ma et al. (2013) used TEMPO/NaBr/NaClO oxidation approach to prepared an aqueous suspension of 0.05wt% ultrafine cellulose nanofiber. The diameter of ultrafine cellulose nanofibers was found to be in the range of 5 to 10 nm, the average aspect ratio of the nanofiber estimated from the Transmission electron microscope (TEM) image was about 160, and the carboxyl group content (1.4mmol/g). The maximum adsorption capacity for $UO_2^{2+}$ could reach167 mg/g due to the chelation between the carboxyl group and $UO_2^{2+}$. After the $UO_2^{2+}$ adsorption, the surface of cellulose nanofibers became covered with metal ionic crystals (Fig. 7). $UO_2^{2+}$ could still be used as a “cross-linker” to convert aqueous CNF into gel.

Prussian blue (PB)(Wang et al. 2018b) is considered to be a promising material due to its excellent adsorption properties and high selectivity for Cs ions. However, the use of PB nanoparticles to remove Cs from a radioactive waste solution is limited by separation problems. Eun et al.(2020) freeze-dried Na-CMCNF solution to obtain CMCNF membrane, and then cross-linked it in $Fe^{3+}$ solution, then reacted with 0.1 or 0.5M potassium hexacyanoferrate (HCF) for rapid synthesis of PB, PB nanoparticles were formed in situ and immobilized at the $Fe^{3+}$ sites of a CMCNF membrane by reaction with HCF, and 0.1M-PB-CMCNF and 0.5M-PB-CMCNF were obtained. (Fig. 8) The PB nanoparticles, which exhibit an irregular morphology, are sparsely distributed on the surface of the 0.1M-PB-CMCNF sample, whereas PB particles densely cover the surface of the 0.5M-PB-CMCNF sample. The removal mechanism of $Cs^{3+}$ due to ion exchange between Cs and K. The 0.5 M-PB-CMCNF membranes exhibited excellent $Cs^{3+}$ uptakes of approximately 130mg/$g_{PB-CMCNF}$.

Anirudhan et al. (2015) used ethylene glycol dimethacrylate (EGDMA) as the crosslinking agent, potassium peroxydisulfate (KPS) as the initiator, Modification of methacrylic acid (MAA) and itaconic acid(IA) in nanocellulose/nanobentonite(NC/NB) composite to obtain PIA/MAA-g-NC/NB(Fig. 9). $U^{6+}$ is removed by ion exchange of carboxyl functional groups. The adsorbent dose is found to be 2.0 g/L for the removal of $U^{6+}$ from 100 mg/L. The simulated nuclear industry wastewater was used to practical efficiency and effectiveness tested, and it was observed that 0.45 g/L adsorbent is sufficient for the complete removal of $U^{6+}$. After 6 adsorption-desorption cycles with 0.1M HCl, a slight decrease in adsorption capacity was observed (from 94.22–89.60%).

Anirudhan et al. (2016) used same adsorbent for the removal of $Co^{2+}$. An adsorbent dose of 2.0 g/L found to be sufficient for the complete removal of $Co^{2+}$ from 100 mg/L at room temperature. After washing with 0.1M HCl solution, it can be carried out 6 adsorption cycles, and will not cause too much loss (from 99.15–88.9%), the adsorbent could be applied in nuclear industrial wastewater.

# 3.6 Adsorbents for other heavy ions

Liu et al.(2014a) compared the adsorption capacity of Ag + on CNC hydrolyzed from cellulose sludge and CNF obtained from grinding. Zeta potential showed negatively charged surfaces for CNC and CNF. The capture of heavy metal ions is accomplished by electrostatic attraction. The presence of $SO_3^-$ groups on the surface of CNC obtained by sulfuric acid hydrolysis has a greater impact on the adsorption of $Ag^+$. The maximum adsorption capacities of CNC and CNF for $Ag^+$ reached 34.4mg/g at pH 6.39 and 15.45 mg/g at pH 5.45, respectively.

Sharma et al.(2018a) used nitric acid/sodium nitrite to oxidize untreated *Australian spinifex grass* to obtain NOCNF, which had low crystallinity of around 50%, high surface charge of -68mV and high hydrophilicity (static contact angle 38°). The suspension (0.20wt%) can remove $Cd^{2+}$ in a large concentration range (50-5000ppm) in a short time (≤ 5min). When the $Cd^{2+}$ concentration is 250ppm, the removal rate can reach 84%. According to the Langmuir curve, the maximum adsorption capacity for $Cd^{2+}$ can reach 2550mg/g.

Arsenic is a metalloid that forms highly toxic compounds in many oxidation states including arsenate ($As^{3+}$) and arsenate ($As^{5+}$). ($As^{3+}$) is reported to be more toxic than ($As^{5+}$) and more difficult to remove from water(Bissen and Frimmel 2003). Zhang et al. (2019) used 1D negatively charged TEMPO-oxidized CNF and positively charged partly deacetylated chitin nanofiber to self-assemble into 3D biohybrid hydrogel (BHH) through electrostatic force at room temperature. Then freeze-drying to obtain biohybrid aerogel (BHA) (Fig. 10). The specific surface area of BHA is 54$m^2$/g, and the maximum adsorption capacity for $As^{3+}$ is 217mg/g.

Chai et al.(2020) used glutaraldehyde as a crosslinking agent to cross link the NC and PEI oxidized by Tempo to obtain NC-PEI/GA nanoparticles. At pH 3, the adsorption equilibrium can be reached within 10min, and the maximum adsorption capacity for $As^{5+}$ is 255.19mg/g. The adsorbent could be easily regenerated and reused via NaOH treatment, and the regeneration efficiency remained relatively steady even after eight cycles.

# 4. Nanocellulose Based Adsorbents For Multiple Heavy Ions Removal

# 4.1 Adsorbents for two heavy ions

Li et al. (2019a) used Tempo to oxidize Hardwood Kraft Pulp and added different amounts of NaClO solutions(150-310g) in the oxidation process to obtain TOCNF with different carboxyl content. The obtained TOCNFs are with typical width of 5–8 nm and length of 1000–2000 nm, carboxylate contents were 0.70, 1.40 and 1.67 mmol/g (TOCNF 0.70/1.40/1.67), respectively. The adsorption process can reach adsorption equilibrium within 2 min. A combined interaction mechanism, including ion exchange,

coordination and accumulation, was proposed based on the study. The maximum adsorption capacity of TOCNF 1.40 on $Cu^{2+}$ and $Zn^{2+}$ was 102.9mg/g and 73.9 mg/g, respectively.

Because the nitrile groups on the surface of polyacrylonitrile (PAN) [108] can react with hydroxylamine in the aqueous solution at room temperature to form amidoxime groups, it has attracted widespread attention in the field of heavy metal ion removal. Yang et al.(2014) obtained oxidized CNFs through Tempo oxidation, were grafted with cysteine to get the thiol group. which were embedded in the electrospun PAN scaffold. The m-CNF membrane has a large surface-to-volume, the thiol group concentration is 0.9mmol/g, and the maximum adsorption capacity for $Cr^{6+}$ and $Pb^{2+}$ is 87.5mg/g and 137.7mg/g, respectively. The m-CNF membrane adsorbed by $Cr^{6+}$ and $Pb^{2+}$ is regenerated by HCl(2M) and EDTA (0.05M) solutions for 3 times. the m-CNF membrane still possessed 93% of the original $Cr^{6+}$ adsorption capacity and 95% of the original $Pb^{2+}$ adsorption capacity.

Since chitosan had strong ability to chelate heavy metal ions due to the amino and hydroxyl groups on its surface(Vakili et al. 2019), Rodrigues et al. (2019) based on chitosan-g-poly(acrylic acid) matrices filled with CNWs to obtain hydrogel composites (Chitosan-g-poly(acrylic acid)/CNWs). The adsorption performance of hydrogels on $Pb^{2+}$ and $Cu^{2+}$ was investigated by controlling the addition amount of CMWS. The highest adsorption of $Pb^{2+}$(818.4 mg/g) and $Cu^{2+}$ (325.5 mg/g) is obtained within 30 min, at pH 4.0, using 20 mg of the hydrogel composite containing 10 w/w-% of CNWs. After washing with 0.1 mol/L HCl solution for five times, the results reveal that the reduction in the amount of metal adsorbed from the first to the last cycle was 10.7% for $Pb^{2+}$ and 18.2% for $Cu^{2+}$, respectively.

Usually, interpenetrating polymer networks(Ding et al. 2020) (IPNs) were composed of two or more different chemical networks that can enhance the mechanical strength of hydrogels. The excellent aspect ratio of NFCs was an ideal material for preparing IPN network hydrogels. Li et al. (2018b) used TEMPO-oxidized NFC and poly(2-(dimethylamino) ethyl methacrylate) (PDMAEMA) to crosslink through free radical polymerization to obtain NFC-PDMAEMAIPNs hydrogel(NPIH). According to the weight of the NFCs and DMAEMA different (0.1 :1, 0.2:1, 0.3:1, 0.4:1, 0.5:1, 0.6:1) the preparation of a series of hydrogel (NPIH-0.1, 0.2, 0.3, 0.4, 0.5, 0.6). These hydrogels possess uniform pore structure and high porosity (> 97%), high surface aera(> 82$m^2$/g) and compressive strength(> 1.26kPa). The adsorption mechanism is chelation of amino group and ion exchange of carboxyl group. The adsorption capacity of NPIH-0.6 is the largest, the maximum adsorption capacity for $Cu^{2+}$ and $Pb^{2+}$ could reach 217.39 and 81.96mg/g, respectively.

Lignin is conjugated polymer with a high consistency of aromatic groups that can interact with cations, moreover, the oxygen-containing groups (the hydroxyl, methoxy, and phenolic groups) are potential interaction sites of lignin for water purification(Naseer et al. 2019). Sirvio et al.(2020) used DES (sulfamic acid and urea) to treat lignin-rich groundwood pulp and sawdust to obtain sulfation of sulfated wood nanofibers (SWNFs) and sulfated sawdust nanofibers (SSDNFs). As A comparison, lignin-free bleached cellulose fibers were treated with the same method to obtain sulfated cellulose nanofibers (SCNFs). The

adsorption capacity of three kinds of nanofibers on $Cu^{2+}$ and $Pb^{2+}$ was investigated. The maximum adsorption capacities of SCNFs for $Cu^{2+}$ and $Pb^{2+}$ were 2.2 and 1.1mmol/g, respectively. However, due to the presence of lignin, the adsorption capacity of SWNFs and SSDNFs was increased to a certain extent. The maximum adsorption capacity of SWNFs for $Cu^{2+}$ and $Pb^{2+}$ is 2.5 and 1.6mmol/g, and the maximum adsorption capacity of SSDNFs for the two are 2.2 and 1.4mmol/g, respectively.

Succinic anhydride is an active agent containing one anhydride group, which can react with the hydroxyl groups of cellulose. Yu et al.(2013) obtained CNCs by hydrolyzing cotton with sulfuric acid, subsequently, CNCs were modified with succinic anhydride, and the product SCNCs were then converted into the sodic form (NaSCNCs). The maximum adsorption capacities of NasCNCs for $Pb^{2+}$ and $Cd^{2+}$ were 465.1 mg/g and 344.8 mg/g, which were higher than those of SCNCs 367.6 mg/g and 259.7 mg/g. NaSCNCs could be efficiently regenerated with a mild saturated NaCl solution with no loss of capacity after two recycles. The adsorption mechanism for SCNCs was a complexation process, while ion-exchange was the principal mechanism for the removal of heavy metal ions from NaSCNCs. Therefore, it was essential to convert the carboxyl groups into carboxylates for this adsorbent containing carboxyl groups.

Clay's high specific surface area, high cation exchange capacity and incredible physical and chemical stability can enhance adsorption(Uddin 2017). Hydroxyapatite(CHA) is an effective adsorbent material due to its capability for simultaneous removal of cationic and anionic contaminants from water(Fernando et al. 2015). Sanna et al. (2018) used NCC as a template, CHA particles and bentonite clay are dispersed in a cellulose matrix to obtain CHA-BENT-NCC particles. The maximum adsorption capacity for $Ni^{2+}$ and $Cd^{2+}$ were 22.96mmol/g, 9.71mmol/g. CHA-BENT-NCC can be regenerated by 0.1M $HNO_3$. After five cycles, the adsorption capacity of CHA-BENT-NCC was decreased from 97–74% for $Cd^{2+}$ and from 98–80% for $Ni^{2+}$.

Li et al.(2018a) obtained the NFC solution through TEMPO oxidation, and then achieved physically-crosslinked network NFC/PEI composite hydrogel(NPH13, NPH22, NPH31) through electrostatic combination with PEI solutions of different weight ratios (1:3, 2:2, 3:1). After freeze-drying, NPA13, NPA22, NPA31 aerogel were obtained. The maximum specific surface area of the aerogel is 42.5$m^2$/g, and it has good shape recover capacity (Fig. 10). The electrostatic attraction and cation exchange between carboxyl and amino groups on $Cu^{2+}$ and $Pb^{2+}$ are the reasons for the high adsorption capacity of aerogels. The maximum adsorption capacities of NPA22 for $Cu^{2+}$ and $Pb^{2+}$ are 175.44mg/g and 357.44mg/g, respectively. After three adsorption/desorption cycles, the adsorption capacity of NPAs still maintained more than 90%.

Yao et al.(2016) used TEMPO-mediated oxidized kraft eucalyptus pulps obtain CNFs hydrogel with carboxylate content (0.65mmol/g). Then Dialdehyde CNFs hydrogel (DACs) was obtained by oxidizing CNFs with NaIO4. CNFs and DACs hydrogels were freeze-dried to obtain porous CNFs and DACs aerogels (Fig. 11). The specific surface area for CNFs and DACs aerogels was 185.1$m^2$/g and 134.4$m^2$/g. In the studied concentration range (0.6–1.0 mmol/L), a removal capacity of 0.75 mmol/g for $Pb^{2+}$ and 0.58

mmol/g for $Cu^{2+}$ was obtained. According to the pseudo-second–order, the theoretical maximum sorption capacity was 38.36 mg/g and 157.73 mg/g for $Cu^{2+}$ and $Pb^{2+}$, respectively.

Derami et al. (2019) incorporated of PDA particles into *Gluconacetobacter hansenii* broth under aerobic and static conditions. PDA particles were grown in situ on the BNC membrane (Fig. 12). The catecholamine group on the surface of PDA particles has a strong affinity to lead ions. Adsorption of PDA/BNC was tested in a mixed solution of $Pb^{2+}$, $Cd^{2+}$. The PDA/BNC membrane removed 5.3 g of $Pb^{2+}$ from water per square meter of the membrane area. The lowest performance was observed for $Cd^{2+}$ with 2.1 g of ions removed per square meter of the membrane area. After regeneration with 0.1M sodium citrate solution, the regenerated membranes exhibited excellent contaminant removal efficiency even after 10 cycles of filtration (about 90% of the initial performance retained).

# 4.2 Adsorbents for three heavy ions

Liu et al.(2015) prepared $CNC_{SL}$ and $CNF_{SL}$ from Cellulose Sludge respectively. Hexokinase enzymes as biocatalysts, grafting the phosphate group of adenosine-5 '-triphosphate (ATP) on $CNF_{SL}$/$CNC_{SL}$, to obtain phos-$CNC_{SL}$ and phos-$CNF_{SL}$ adsorbent. As a contrast, nanocrystals ($CNC_{BE}$) prepared by bioethanol were also used to investigate the adsorption capacity of $Ag^{+}$, $Cu^{2+}$ and $Fe^{3+}$. The results showed that the maximum adsorption capacities of Phos-$CNF_{SL}$ for $Ag^{+}$, $Cu^{2+}$ and $Fe^{3+}$ were 120,114,73, which were all lower than the 136,117,115 of Phos-$CNC_{SL}$. It can remove more than 99% of $Cu^{2+}$ and $Fe^{3+}$ in the wastewater in the mirror making industry.

It was evident that tannins had a high chelating affinity for heavy metal ions due to its large number of adjacent phenolic hydroxyls content(Bacelo et al. 2016). Xu et al. (2017) used sulfuric acid to hydrolyze bleached kraft pulp to obtain NCC, and then oxidized NCC with sodium periodate to obtain dialdehyde nanocellulose (DANC), and then generated TNCC by reacting the aldehyde group on the DANC with the reactive hydrogen on the tannin molecule. DANC can be used as matrix and crosslinker. The adsorption mechanism is the strong complexing ability of phenolic hydroxyl groups on metal ions, on the other hand, ionization can enhance the electrostatic attraction ability of metal cations and anions TNCC. Calculated according to Sips model, the maximum adsorption capacities of TNCC for $Cu^{2+}$, $Pb^{2+}$, and $Cr^{6+}$ are 51.846, 53.371 and 104.592mg/g, respectively. The results showed that the maximum adsorption capacities of TNCC for $Cu^{2+}$, $Pb^{2+}$, and $Cr^{6+}$ are 49.140, 49.530 and 103.259mg/g. After 5 times of adsorption-desorption using 0.1M $HNO_3$ solution, the adsorption capacity of TNCC for $Cu^{2+}$ and $Pb^{2+}$ could still reach 43.12 and 45.69mg/g. However, the adsorption capacity(1.06mg/g) for $Cr^{6+}$ decreased greatly even after the first regeneration. The poor adsorption performance of TNCC after regeneration may be attributed to its redox adsorption for $Cr^{6+}$.

Feng et al. (2018) used electronspinning technique to prepare PAN/CA (cellulose acetate) composite nanofibrous membranes, and then amidoxime ployarcylonitrile/regenerate cellulose (AOPAN/RC) composite nanofibrous membranes were prepared by combining hydrolysis and amidoximation

modification(Fig. 13). CA can be dissolved in a variety of solvents, so it can become nanofibers through electrospun. The adsorption mechanism of the membrane is coordination/chelation between metal ions and amidoxime/hydroxyl groups. The maximum adsorption capacity of AOPAN/RC for $Fe^{3+}$, $Cu^{2+}$ and $Cd^{2+}$ are 7.47, 4.26, 1.13 mmol/g, respectively. After 5 adsorption/desorption experiments, its adsorption rate could still retain more than 80%.

Shahnaz et al. (2020b) hydrolyzed cellulose with sulfuric acid and oxidized sodium periodate to obtain dialdehyde-based nanocellulose (DANC). Bentonite was converted into NB under ultrasound. Chitosan was modified with chloroacetic acid to obtain carboxymethyl chitosan. CMC, DANC and NB are mixed to obtain hydrogel slurry, which is freeze-dried to obtain the nanobentonite incorporated dialdehyde nanocellulose-carboxymethyl chitosan aerogel (NBNC). The response surface methodology (RSM) method was used to analyze the optimal reaction conditions of NBNC to heavy metal ions. The adsorption capacity for $Cr^{6+}$, $Co^{3+}$ and $Cu^{2+}$ are 2749.68, 916.65, and 1937.49 mg/g, respectively.

Polyurethane (PU)(Kalaivani et al. 2016) has the advantages of high mechanical strength and stability, and high specific surface area under different environmental conditions, and can be applied to the adsorption of heavy metal ions. Hong et al.(2018) filled different concentrations of CMCNFs (2,3,4 wt%) in PU foam as filler to obtain PU/CMCNF(neat-PU, PU/CMCNF-2,3,4) foams. SEM images show that the surface of the composite foam material is rough and porous (Fig. 14). The maximum adsorption capacities of CMCNF embedded in PU foam were found to be 78.7 mg/g and 216.1 mg/g for $Cu^{2+}$ and $Pb^{2+}$ removal, respectively, in PU/CMCNF-2, while PU/CMCNF-3 exhibited maximum removal capacity for $Cd^{2+}$ (98 mg/g).

Magnetic separation technology is widely used in separation and purification. Super magnetic ion materials include Ni, Co, Fe, $Fe_2O_3$, $Fe_3O_4$, Fe-Co, and Ni-Fe (Zhu et al. 2011). Among them, $Fe_3O_4$ nano-ion is stable and widely used in culture mediums due to its low toxicity. Zhu et al. (2011) synthesized BC from *Xylobacteria* by agitated fermentation method, and biosynthesized spherical $Fe_3O_4$/BC nanocomposite by pH-controlled embedding method. The maximum adsorption capacities of $Fe_3O_4$/BC spheres for $Pb^{2+}$, $Mn^{2+}$ and $Cr^{3+}$ are 65, 33 and 25mg/g, respectively. Since the superparamagnetic spherical $Fe_3O_4$/BC nanocomposites are recycled using magnetic field separation, it can be utilized repeatedly. After recycling with 0.1mol/L sodium citrate, the adsorption capacity of $Fe_3O_4$/BC spheres for the three ions decreased slightly.

Hosseini et al.(2020) prepared CNFs from date palm tree waste, cellulose nanofibrills cryogels modified with 10% GO and 10% $Fe_3O_4$ nanoparticle as filler (CNFs/GO/$Fe_3O_4$) were prepared by facile freeze-drying methodology. CNF can enhance the mechanical strength and adsorption capacity of the adsorbent. The CNFs/GO/$Fe_3O_4$ cryogels has a low density of 0.0139g/$cm^3$ and an ultra-porosity of 99.46%, appropriate specific surface area ($S_{BET}$=55$m^2$/g), the maximum adsorption capacity of the CNFs/GO/$Fe_3O_4$ cryogels for $Pb^{2+}$, $Hg^{2+}$, $Cr^{6+}$ at 298±°1 K are 126.58, 36.7 and 73.52mg/g, respectively.

Anirudhan et al.(2015b) used EGDMA as a crosslinking agent and $K_2S_2O_8$ as a free radical initiator, and it was grafted onto magnetite nanocellulose by itaconic acid, and then further modified by 2-mercaptobenzamide to obtain a new type of thiol and carboxyl functionalized magnetite nanocellulose composite particle (P(MB-IA)-g-MNCC) to remove $Hg^{2+}$ in chlor-alkali industrial wastewater. $Hg^{2+}$ is removed by the ion exchange of carboxyl groups and the complexation of thiol groups, and its maximum adsorption capacity is 240.0mg/g. They used the same adsorbent to remove $Cd^{2+}$(Anirudhan and Shainy 2015a) and $Co^{2+}$(Anirudhan et al. 2019), its maximum adsorption capacity is 262.27mg/g and 349.62mg/g, respectively.

# 4.3 Adsorbents for four heavy ions

Zheng et al. (2014) used eucalyptus kraft pulp for TEMPO oxidation to obtain CNFs, and then used glutaraldehyde as a cross-linking agent, cross-linked PVA and CNFs and then freeze-dried to obtain PVA/CNF aerogels, and then used methyltrichlorosilane to pass thermal chemical vapor After the deposition process, the silane-coated PVA/CNF aerogel is obtained, which has super-hydrophobic and superoleophilic capabilities (Fig. 15). The porosity of all aerogels is over than 98%. The carboxyl groups in the porous material have electrostatic attraction and chelation for heavy metal ions. The maximum adsorption capacity of PVA/CNF aerogel for $Hg^{2+}$, $Pb^{2+}$, $Cu^{2+}$ and $Ag^{+}$ is 157.5, 22, 110.6 and 24.5mg/g, respectively. The silane-coated PVA/CNF aerogel can be used to clean up oil/chemical spills/leaks contamination.

Carbon dots(CDs) have caused extensive research due to their chemical stability, excellent biocompatibility, non-toxicity and colorful photoluminescence(Zhou et al. 2018). Guo et al. (2019) obtained Carboxymethylated Cellulose Nanofibrils (CM-CMFs) after carboxymethylated Eucalyptus Kraft Pulp by sodium hydroxide/chloroacetic acid treatment and homogenization. The CM-CNFs were further modified with CDs based on a typical condensation reaction. A series of fluorescent nano cellulosic hydrogels (FNH-1, 2, 3, 4, 5, 6) were prepared through radical polymerization of CM-CNF-CDs, AA, AM and MBA (0.01, 0.02, 0.1, 0.55, 1.00, 1.45wt%) by using PPS as the initiator. High content of amino, hydroxyl, and carboxyl groups can provide adsorption sites, and the 3D network structure of the hydrogel promotes the adsorption of metal ions from the outside to the inside. The maximum adsorption capacity of the FNH-5 for $Fe^{3+}$, $Ba^{2+}$, $Pb^{2+}$ and $Cu^{2+}$ ions was tested, and they were 769 mg/g, 212 mg/g, 2056 mg/g, 1246 mg/g, respectively.

Hokkanen et al.(2013) used succinic anhydride to modify mercerized nanocellulose through succinylation reaction, and obtained a carboxyl-containing adsorbent. The SEM image showed that after the modification, the crystallinity increased significantly. Fourier Transform Infrared (FTIR) results show that there are carboxyl groups on the surface of the adsorbent. $Co^{2+}$, $Ni^{2+}$, $Cu^{2+}$, $Zn^{2+}$ and $Cd^{2+}$ can be effectively removed by ion exchange. The adsorption capacities of Mercerized Nanocellulose were 1.338, 0.744, 1.900, 1.610, 2.062mmol/g, respectively. Recycling of adsorbent can be realized by nitric acid and ultrasonic treatment with regeneration efficiencies ranging from 96–100%.

# Conclusions And Perspectives

As an emerging materials platform for heavy metal ions removal, nanocellulose based adsorbents exhibit many advantages, but challenges are to be properly resolved in the future (Fig. 16). For instance, given strong negative ion groups, nanocellulose based adsorbents have a high electrostatic attraction ability, offering desired adsorbing sites for heavy metal ions. However, hydrophilic negative ion groups will decrease the hydrophobic ability and stability of the adsorbents in water. Possible solutions are, but not limited to, modifying the nanocellulose or integrating assemble processes to enhance the crosslinking behaviors among nanocellulose and the other furnishes.

Surface modifications of nanocellulose, such as, oxidation, phosphorylation and amination, could promote the adsorbing sites of nanocellulose based adsorbents, but likely result in the rapid decrease of their desorption ability. To increase the recycling times of adsorbents, more acid washing is required, which will also cause harm to the environment. To obtain the high desorption capacities, we can firstly try to find some groups which have different binding affinity for heavy metal ions, then assemble these groups into the multilayer 2D/3D nanocellulose based adsorbent aerogels or composites, finally prepare the high adsorption/desorption ability adsorbents.

To meet the requirements of recycling, selective adsorptions or desorption for different heavy metal ions, precisely controlled assembles of nanocellulose based adsorbents with tailorable hydrophilicities and mechanical properties are desired for the industrial applications. For example, to optimize the assembling process, crosslinking agent and functional additive kinds in adsorbent networks have to be properly selected to modulate the suitable porous structures and adsorption capacities. In addition, computational modeling and advanced in situ characterizations would be beneficial, which, in turn, will further guide researchers to the rational design of cellulose-based adsorbents for heavy metal ions removal.

# Abbreviations

| NC | Nanocellulose |
|---|---|
| NFCs | Nanofibrillated cellulose |
| BNCs | Bacteria nanocellulose |
| CNCs | Cellulose nanocrystals |
| SEM | Scanning electron microscope |
| TEMPO | 2,2,6,6-Tetramethyl-1-piperidinyloxy |
| CMCNFs | Carboxymethylation CNFs |
| MA | Maleic anhydride |
| TA | Tannic acid |
| CDA | Cardanol-derived siloxane |
| BET | Brunner – Emmet – Teller |
| PEI | Polyethyleneimine |
| GPTMS | 3-glycidyloxypropyl trimethoxy silane |
| TMPTAP | Trimethylolpropane-tris-(2-methy-1-aziridine) propionate |
| TO-CTP | TO-CNF/TMPTAP/PEI |
| GA | Glutaraldehyde |
| PDA | Polydopamine |
| PAA | Peracetic acid |
| CNS | Cellulose nanosheet |
| GO | Graphene oxide |
| CF | Composite fiber |
| Alg | alginate |
| AC | Activated carbon |
| BA | Butyl acrylate |
| PVA | Polyvinyl alcohol |
| m-CS | Magnetic chitosan |
| SINC | Sodium itaconate grafted nanocellulose |
| c-DAC | Cationic dialdehyde cellulose |
| EDA | Ethylenediamine |

| NC | Nanocellulose |
|---|---|
| PAMAM | Poly(amidoamine) |
| MPA | Mercaptopropionic acid |
| PPY | Polypyrrole |
| LNFs | Lysozyme nanofibrils |
| HSAB | Hard-soft acid base |
| MPTMS | 3-mercaptopropyltrimethoxysilane |
| SNC | Spherical nanocellulose |
| 3-MPA | 3-mercaptopropionic acid |
| $^{13}$C-NMR | Nuclear magnetic resonance |
| Cys | Cysteamine |
| TEM | Transmission electron microscope |
| PB | Prussian blue |
| HCF | Hexacyanoferrate |
| EGDMA | Ethylene glycol dimethacrylate |
| KPS | Potassium peroxydisulfate |
| MAA | Methacrylic acid |
| IA | Itaconic acid |
| NB | Nanobentonite |
| BHH | Biohybrid hydrogel |
| BHA | Biohybrid aerogel |
| PAN | Polyacrylonitrile |
| IPNs | Interpenetrating polymers networks |
| PDMAEMA | Poly(2-(dimethylamino) ethyl methacrylate) |
| SWNFs | Sulfated wood nanofibers |
| SSDNFs | Sulfated sawdust nanofibers |
| SCNFs | Sulfated cellulose nanofibers |
| CHA | hydroxyapatite |
| NPH | NFC/PEI composite hydrogel |

| NC | Nanocellulose |
|---|---|
| ATP | Adenosine-5’-triphosphate |
| CA | Cellulose acetate |
| AOPAN/RC | Amidoxime polyacrylonitrile/ regenerate cellulose |
| RSM | Response surface methodology |
| PU | Polyurethane |
| CDs | Carbon dots |
| FNH | Fluorescent nanocellulosic hydrogels |
| FTIR | Fourier Transform Infrared |

# Declarations

**Authors’ contributions**: All authors contributed as the main contributors of this work. All authors performed the literature search and analysis. All authors had drafted, revised the work and approved the final paper.

**Funding:** This article was financially supported by the National Key R&D Program of China (2017YFB0307900).

**Availability of data and material:** Not applicable.

**Code availability:** Not applicable.

**Compliance with Ethical Standards**

**Conflict of Interest:** The authors declare that they have no conflict of interest.

**Ethical approval:** This article does not contain any studies with human participants or animals performed by any of the authors.

# References

1. Anetor JI (2012) Rising Environmental Cadmium Levels in Developing Countries: Threat to Genome Stability and Health Nigerian journal of physiological ences: official. publication of the Physiological Society of Nigeria 27:103–115. doi:10.4172/2161-0525.1000140
2. Anirudhan TS, Deepa JR, Binusreejayan (2015) Synthesis and characterization of multi-carboxyl-functionalized nanocellulose/nanobentonite composite for the adsorption of uranium(VI) from aqueous solutions: Kinetic and equilibrium profiles. Chem Eng J 273:390–400. doi:10.1016/j.cej.2015.03.007

3. Anirudhan TS, Deepa JR, Christa J (2016) Nanocellulose/nanobentonite composite anchored with multi-carboxyl functional groups as an adsorbent for the effective removal of Cobalt(II) from nuclear industry wastewater samples. Journal of Colloid Interface ence 467:307–320. doi:10.1016/j.jcis.2016.01.023
4. Anirudhan TS, Shainy F (2015a) Adsorption behaviour of 2-mercaptobenzamide modified itaconic acid-grafted-magnetite nanocellulose composite for cadmium(II) from aqueous solutions. J Ind Eng Chem 32:157–166. doi:10.1016/j.jiec.2015.08.011
5. Anirudhan TS, Shainy F (2015b) Effective removal of mercury(II) ions from chlor-alkali industrial wastewater using 2-mercaptobenzamide modified itaconic acid-grafted-magnetite nanocellulose composite. J Colloid Interface Sci 456:22–31. doi:10.1016/j.jcis.2015.05.052
6. Anirudhan TS, Shainy F, Deepa JR (2019) Effective removal of Cobalt(II) ions from aqueous solutions and nuclear industry wastewater using sulfhydryl and carboxyl functionalised magnetite nanocellulose composite: batch adsorption studies. Chem Ecol 35:235–255. doi:10.1080/02757540.2018.1532999
7. Attia AA, Khedr SA, Elkholy SAJBJoCE (2010) Adsorption of chromium ion (VI) by acid activated carbon Brazilian. Journal of Chemical Engineering 27:183–193
8. b HPSAKa AYD, C MNIA, A AM, D KS ERDA, B MJ (2014) Production and modification of nanofibrillated cellulose using various mechanical processes. A review Carbohydrate Polymers 99:649–665. doi:10.1016/j.carbpol.2013.08.069
9. Bacelo HAM, Santos SCR, Botelho CMS (2016) Tannin-based biosorbents for environmental applications-A review. Chem Eng J 303:575–587. doi:10.1016/j.cej.2016.06.044
10. Bissen M, Frimmel FHJCSAW (2003) Arsenic — a Review. Part II: Oxidation of Arsenic and its Removal in Water Treatment 31:97–107
11. Buesseler KO et al (2012) Fukushima-derived radionuclides in the ocean and biota off Japan. Proc Natl Acad Sci U S A 109:5984–5988. doi:10.1073/pnas.1120794109
12. Chai F, Wang RK, Yan LL, Li GH, Cai YY, Xi CY (2020) Facile fabrication of pH-sensitive nanoparticles based on nanocellulose for fast and efficient As(V) removal Carbohydrate Polymers 245 doi:10.1016/j.carbpol.2020.116511
13. Chauhan] GS (2018) New spherical nanocellulose and thiol-based adsorbent for rapid and selective removal of mercuric ions. Chem Eng J 331:587–596. doi:10.1016/j.cej.2017.08.128
14. Chen LH, Zhu JY, Baez C, Kitin P, Elder T (2016) Highly thermal-stable and functional cellulose nanocrystals and nanofibrils produced using fully recyclable organic acids. Green Chem 18:3835–3843. doi:10.1039/c6gc00687f
15. Cui LM, Wang YG, Gao L, Hu LH, Yan LG, Wei Q, Du B (2015) EDTA functionalized magnetic graphene oxide for removal of Pb(II), Hg(II) and Cu(II) in water treatment: Adsorption mechanism and separation property. Chem Eng J 281:1–10. doi:10.1016/j.cej.2015.06.043
16. Derami HG et al (2019) A Robust and Scalable Polydopamine/Bacterial Nanocellulose Hybrid Membrane for Efficient Wastewater Treatment Acs. Applied Nano Materials 2:1092–1101.

doi:10.1021/acsanm.9b00022

17. Ding HY, Liang XX, Wang Q, Wang MM, Li ZJ, Sun GX (2020) A semi-interpenetrating network ionic composite hydrogel with low modulus, fast self-recoverability and high conductivity as flexible sensor. Carbohyd Polym 248:11. doi:10.1016/j.carbpol.2020.116797
18. Du HS, Liu C, Zhang YD, Yu G, Si CL, Li B (2016) Preparation and characterization of functional cellulose nanofibrils via formic acid hydrolysis pretreatment and the followed high-pressure homogenization. Ind Crop Prod 94:736–745. doi:10.1016/j.indcrop.2016.09.059
19. Du L et al (2018) Increased Iron Deposition on Brain Quantitative Susceptibility Mapping Correlates with Decreased Cognitive Function in Alzheimer's Disease. ACS Chem Neurosci 9:1849–1857. doi:10.1021/acschemneuro.8b00194
20. El-Saied H, Basta AH, Gobran RH (2004) Research Progress in Friendly Environmental Technology for the Production of Cellulose Products (Bacterial Cellulose and Its Application. Polymer-Plastics Technology Engineering 43:797–820. doi:10.1081/PPT-120038065
21. Eldin et al (2016) Development of amphoteric alginate/aminated chitosan coated microbeads for oral protein delivery International. Journal of Biological Macromolecules: Structure Function Interactions 92:362–370. doi:10.1016/j.ijbiomac.2016.07.019
22. Eun S, Hong HJ, Kim H, Jeong HS, Kim S, Jung J, Ryu J (2020) Prussian blue-embedded carboxymethyl cellulose nanofibril membranes for removing radioactive cesium from aqueous solution Carbohydrate Polymers 235 doi:10.1016/j.carbpol.2020.115984
23. Fan XM, Yu HY, Wang DC, Mao ZH, Yao JM, Tam KC (2019) Facile and Green Synthesis of Carboxylated Cellulose Nanocrystals as Efficient Adsorbents in Wastewater Treatments. ACS Sustain Chem Eng 7:18067–18075. doi:10.1021/acssuschemeng.9b05081
24. Feng Q, Wu D, Zhao Y, Wei A, Wei Q, Fong H (2018) Electrospun AOPAN/RC blend nanofiber membrane for efficient removal of heavy metal ions from water. J Hazard Mater 344:819–828. doi:10.1016/j.jhazmat.2017.11.035
25. Feng YA et al (2010) Adsorption of Cd (II) and Zn (II) from aqueous solutions using magnetic hydroxyapatite nanoparticles as adsorbents. Chem Eng J 162:487–494. doi:10.1016/j.cej.2010.05.049
26. Fernando MS, Silva RMD, Silva KMNDJASe (2015) Synthesis, characterization, and application of nano hydroxyapatite and nanocomposite of hydroxyapatite with granular activated carbon for the removal of Pb2 + from aqueous solutions. Appl Surf Sci 351:95–103. doi:10.1016/j.apsusc.2015.05.092
27. Ferreira-Neto EP, Phd SU, Silva TCDA, Domeneguetti RR, Ribeiro S (2020) Bacterial nanocellulose/MoS2 hybrid aerogels as bifunctional adsorbent/photocatalyst membranes for in-flow water decontamination. ACS Applied Materials Interfaces 12:41627–41643. doi:10.1021/acsami.0c14137
28. Fu F, Wang Q (2011) Removal of heavy metal ions from wastewaters: a review. J Environ Manage 92:407–418. doi:10.1016/j.jenvman.2010.11.011

29. Gan PG, Sam ST, Abdullah MF, Omar MF, Tan LSJB (2020) An Alkaline Deep Eutectic Solvent Based on Potassium Carbonate and Glycerol as Pretreatment for the Isolation of Cellulose Nanocrystals from Empty. Fruit Bunch Bioresources 15:1154–1170. doi:10.15376/biores.15.1.1154-1170
30. Garba ZN, Lawan I, Zhou W, Zhang M, Wang L, Yuan Z (2020) Microcrystalline cellulose (MCC) based materials as emerging adsorbents for the removal of dyes and heavy metals -. A review Science of the Total Environment 717. doi:10.1016/j.scitotenv.2019.135070
31. Geng B et al (2017) Surface-Tailored Nanocellulose Aerogels with Thiol-Functional Moieties for Highly Efficient and Selective Removal of Hg(II) Ions from Water ACS Sustainable Chemistry and Engineering:11715–11726
32. Guo X, Xu D, Yuan H, Luo Q, Tang S, Liu L, Wu Y (2019) A novel fluorescent nanocellulosic hydrogel based on carbon dots for efficient adsorption and sensitive sensing in heavy metals. Journal of Materials Chemistry A 7:27081–27088. doi:10.1039/c9ta11502a
33. Han KN, Yu BY, Kwak SY (2012) Hyperbranched poly(amidoamine)/polysulfone composite membranes for Cd(II) removal from water. J Membr Sci 396:83–91. doi:10.1016/j.memsci.2011.12.048
34. He J, Zhao H, Li X, Su D, Zhang F, Ji H, Liu R (2018) Superelastic and superhydrophobic bacterial cellulose/silica aerogels with hierarchical cellular structure for oil absorption and recovery. J Hazard Mater 346:199–207. doi:10.1016/j.jhazmat.2017.12.045
35. Hernandez-Francisco E et al (2020) Entangled cellulose nanofibrils/nanosheets derived from native mexican agave for lead(II). ion removal Cellulose 27:8785–8798. doi:10.1007/s10570-020-03373-6
36. Hokkanen S, Repo E, Sillanp?? MJCEJ (2013) Removal of heavy metals from aqueous solutions by succinic anhydride modified mercerized nanocellulose. Chem Eng J 223:40–47. doi:10.1016/j.cej.2013.02.054
37. Hong HJ, Lim JS, Hwang JY, Kim M, Jeong HS, Park MS (2018) Carboxymethlyated cellulose nanofibrils(CMCNFs) embedded in polyurethane foam as a modular adsorbent of heavy metal ions. Carbohyd Polym 195:136–142. doi:10.1016/j.carbpol.2018.04.081
38. Hosseini M, Dizaji HZ, Taghavi M, Babaei AA (2020) Preparation of ultra-lightweight and surface-tailored cellulose nanofibril composite cryogels derived from Date palm waste as powerful and low-cost heavy metals adsorbent to treat aqueous medium. Ind Crop Prod 154:13. doi:10.1016/j.indcrop.2020.112696
39. Hu ZH, Omer AM, Ouyang Xk, Yu DJIJoBM (2018) Fabrication of carboxylated cellulose nanocrystal/sodium alginate hydrogel beads for adsorption of Pb(II) from aqueous solution. Int J Biol Macromol 108:149–157. doi:10.1016/j.ijbiomac.2017.11.171
40. Huang X, Dognani G, Hadi P, Yang M, Hsiao BS Removal (2020) Cationic Dialdehyde Nanocellulose from Sugarcane Bagasse for Efficient Chromium(VI). ACS Sustainable Chemistry Engineering 12:4734–4744. doi:10.1021/acssuschemeng.9b06683
41. İlayda D, Duygu, Ege A, Reza K (2016) Graphene oxides for removal of heavy and precious metals from wastewater. Journal of Materials Science 51:6097–6116. doi:10.1007/s10853-016-9913-8

42. Isogai A (2020) Emerging Nanocellulose Technologies. Recent Developments Advanced Materials. doi:10.1002/adma.202000630
43. Ji Y, Wen YY, Wang Z, Zhang SF, Guo MJ (2020) Eco-friendly fabrication of a cost-effective cellulose nanofiber-based aerogel for multifunctional applications in Cu(II) and organic pollutants removal. J Clean Prod 255:11. doi:10.1016/j.jclepro.2020.120276
44. Jordan JH, Easson MW, Condon BD (2019) Alkali Hydrolysis of Sulfated Cellulose Nanocrystals: Optimization of Reaction Conditions and Tailored. Surface Charge Nanomaterials 9:15. doi:10.3390/nano9091232
45. Juntao et al (2019) Compressible cellulose nanofibril (CNF) based aerogels produced via a bio-inspired strategy for heavy metal ion and dye removal. Carbohyd Polym 208:404–412. doi:10.1016/j.carbpol.2018.12.079
46. Kalaivani SS, Muthukrishnaraj A, Sivanesan S, Ravikumar L (2016) Novel hyperbranched polyurethane resins for the removal of heavy metal ions from aqueous solution Process. Saf Environ Protect 104:11–23. doi:10.1016/j.psep.2016.08.010
47. Kardam A, Raj KR, Srivastava S, Srivastava MM (2014) Nanocellulose fibers for biosorption of cadmium, nickel, and lead ions from aqueous solution. Clean Technologies Environmental Policy 16:385–393. doi:10.1007/s10098-013-0634-2
48. Larsson PA, Berglund LA, W?Gberg L (2014) Ductile all-cellulose nanocomposite films fabricated from core-shell structured. cellulose nanofibrils Biomacromolecules 15:2218–2233. doi:10.1021/bm500360c
49. Lee N, Liu ML, Wu MC, Chen TH, Hou CH (2021) The effect of redox potential on the removal characteristic of divalent cations during activated carbon-based capacitive. deionization Chemosphere 274:9. doi:10.1016/j.chemosphere.2021.129762
50. Lei Y, Qian X, Shen J, An X (2012) Integrated Reductive/Adsorptive Detoxification of Cr(VI)-Contaminated Water by Polypyrrole/Cellulose Fiber. Composite Industrial Engineering Chemistry Research 51:10408–10415. doi:10.1021/ie301136g
51. Lei Z, Gao W, Zeng J, Wang B, Xu J (2019) The mechanism of Cu (II) adsorption onto 2,3-dialdehyde nano. -fibrillated celluloses Carbohydrate Polymers doi:10.1016/j.carbpol.2019.115631
52. Li et al (2018a) Shape memory aerogels from nanocellulose and polyethyleneimine as a novel adsorbent for removal of Cu(II) and Pb(II). Carbohyd Polym 196:376–384. doi:10.1016/j.carbpol.2018.05.015
53. Li J, Xu Z, Wu W, Jing Y, Dai H, Fang G (2018b) Nanocellulose/Poly(2-(dimethylamino)ethyl methacrylate)Interpenetrating polymer network hydrogels for removal of Pb(II) and Cu(II) ions Colloids Surfaces. A Physicochemical Engineering Aspects 538:474–480. doi:10.1016/j.colsurfa.2017.11.019
54. Li MY, Messele SA, Boluk Y, El-Din MG (2019a) Isolated cellulose nanofibers for Cu (II) and Zn (II) removal: performance and mechanisms. Carbohyd Polym 221:231–241. doi:10.1016/j.carbpol.2019.05.078

55. Li P, Sirvi? JA, Haapala A, Liimatainen H (2017) Cellulose Nanofibrils from Nonderivatizing Urea-Based Deep Eutectic Solvent Pretreatments Acs. Appl Mater Interfaces 9:2846–2855. doi:10.1021/acsami.6b13625
56. Li W, Ju B, Zhang S (2019b) Preparation of cysteamine-modified cellulose nanocrystal adsorbent for removal of mercury ions from. aqueous solutions Cellulose 26:4971–4985. doi:10.1007/s10570-019-02420-1
57. Li W, Wang R, Liu SJPiC (2010) Preparation of Nanocrystalline Cellulose Progress in Chemistry 22:2060–2070
58. Liu P, Borrell PF, Bo?i? M, Kokol V, Oksman K, Mathew AP (2015) Nanocelluloses and their phosphorylated derivatives for selective adsorption of Ag+, Cu2 + and Fe3 + from industrial effluents. J Hazard Mater 294:177–185. doi:10.1016/j.jhazmat.2015.04.001
59. Liu P, Oksman K, Mathew AP (2016) Surface adsorption and self-assembly of Cu(II) ions on TEMPO-oxidized cellulose nanofibers in aqueous media. J Colloid Interface Sci 464:175–182. doi:10.1016/j.jcis.2015.11.033
60. Liu P, Sehaqui H, Tingaut P, Wichser A, Oksman K, Mathew AP (2014a) Cellulose and chitin nanomaterials for capturing silver ions (Ag+) from water via. surface adsorption Cellulose 21:449–461. doi:10.1007/s10570-013-0139-5
61. Liu Q, Yuan T, Fu QJ, Bai YY, Yao CL (2019) Choline chloride-lactic acid deep eutectic solvent for delignification and nanocellulose production of. moso bamboo Cellulose 26:9447–9462. doi:10.1007/s10570-019-02726-0
62. Liu R et al (2011) Dopamine as a Carbon Source: The Controlled Synthesis of Hollow Carbon Spheres and Yolk-Structured Carbon Nanocomposites Angew. Chem-Int Edit 50:6799–6802. doi:10.1002/anie.201102070
63. Liu Y, Wang H, Yu G, Yu Q, Li B, Mu X (2014b) A novel approach for the preparation of nanocrystalline cellulose by using phosphotungstic. acid Carbohydrate Polymers 110:415–422. doi:10.1016/j.carbpol.2014.04.040
64. Ma H, Hsiao BS, Chu BJAML (2013) Ultrafine Cellulose Nanofibers as Efficient Adsorbents for Removal of UO22 + in. Water Acs Macro Letters 1:213–216. doi:10.1021/mz200047q
65. Mautner A, Maples HA, Kobkeatthawin T, Kokol V, Karim Z, Li K, Bismarck A (2016) Phosphorylated nanocellulose papers for copper adsorption from aqueous solutions International. Journal of Environmental Science Technology 13:1861–1872. doi:10.1007/s13762-016-1026-z
66. Miretzky P, Cirelli AF (2009) Hg(II) removal from water by chitosan and chitosan derivatives: A review J Hazard Mater 167:10–23 doi:10.1016/j.jhazmat.2009.01.060
67. Mo L (2019) 3D multi-wall perforated nanocellulose-based polyethylenimine aerogels for ultrahigh effcient and reversible removal of Cu(2+) ions from water Chem Eng J 378 doi:10.1016/j.cej.2019.122157
68. Naduparambath et al (2018) Isolation and characterisation of cellulose nanocrystals from sago seed shells. Carbohyd Polym 180:13–20. doi:10.1016/j.carbpol.2017.09.088

69. Naseer A et al (2019) Lignin and Lignin Based Materials for the Removal of Heavy Metals from Waste Water-An Overview Z Phys Chemie-Int. J Res Phys Chem Chem Phys 233:315–345. doi:10.1515/zpch-2018-1209
70. Ninomiya K et al (2018) Lignocellulose nanofibers prepared by ionic liquid pretreatment and subsequent mechanical nanofibrillation of bagasse powder: Application to esterified bagasse/polypropylene composites. Carbohyd Polym 182:8–14. doi:10.1016/j.carbpol.2017.11.003
71. Park JH, Kim H, Kim M, Lim JM, Ryu J, Kim S (2020) Sequential removal of radioactive Cs by electrochemical adsorption and desorption reaction using core-shell structured carbon nanofiber-Prussian blue composites. Chem Eng J 399:10. doi:10.1016/j.cej.2020.125817
72. Petrova MV, Ourgaud M, Boavida JRH, Dufour A, Onrubia JAT, Lozingot A, Heimburger-Boavida LE (2020) Human mercury exposure levels and fish consumption at the. French Riviera Chemosphere 258:7. doi:10.1016/j.chemosphere.2020.127232
73. Qin FM et al (2019a) Efficient Removal of Cu2 + in Water by Carboxymethylated Cellulose Nanofibrils. Performance Mechanism Biomacromolecules 20:4466–4475. doi:10.1021/acs.biomac.9b01198
74. Qin H, Hu T, Zhai Y, Lu N, Aliyeva J (2019b) The improved methods of heavy metals removal by biosorbents: A review Environmental Pollution 258 doi:10.1016/j.envpol.2019.113777
75. Ram B, Chauhan GS, Mehta A, Gupta R, Chauhan K (2018) Spherical nanocellulose-based highly efficient and rapid multifunctional naked-eye Cr(VI) ion chemosensor and adsorbent with mild antimicrobial properties. Chem Eng J 349:146–155. doi:10.1016/j.cej.2018.05.085
76. Rani K, Gomathi T, Vijayalakshmi K, Saranya M, Sudha PN (2019) Banana fiber Cellulose Nano Crystals grafted with butyl acrylate for heavy metal lead (II) removal. Int J Biol Macromol 131:461–472. doi:10.1016/j.ijbiomac.2019.03.064
77. Rodrigues FHA, Magalhães CEdC, Medina AL, Cellulose ARFJ (2019) Hydrogel composites containing nanocellulose as adsorbents for aqueous removal of heavy metals: design, optimization. and application Cellulose 26:9119–9133. doi:10.1007/s10570-019-02736-y
78. Rong LD et al (2018) Facile fabrication of thiol-modified cellulose sponges for adsorption of Hg2 + from. aqueous solutions Cellulose 25:3025–3035. doi:10.1007/s10570-018-1758-7
79. Saito T, Kimura S, Nishiyama Y, Isogai A (2007) Cellulose nanofibers prepared by TEMPO-mediated oxidation of. native cellulose Biomacromolecules 8:2485. doi:10.1021/bm0703970
80. Sanna H, Amit B, Varsha S, Valtteri S, Mika S (2018) Removal of Cd 2+, Ni 2 + and PO 4 3 from aqueous solution by hydroxyapatite-bentonite clay-nanocellulose composite. Int J Biol Macromol 118:903–912. doi:10.1016/j.ijbiomac.2018.06.095
81. Sari AA et al (2017) Mechanism, adsorption kinetics and applications of carbonaceous adsorbents derived from black liquor sludge. J Taiwan Inst Chem Eng 77:236–243. doi:10.1016/j.jtice.2017.05.008
82. Septevani AA, Rifathin A, Sari AA, Sampora Y, Ariani GN, Sudiyarmanto, Sondari D (2020) Oil palm empty fruit bunch-based nanocellulose as a super-adsorbent for water remediation Carbohydrate

Polymers 229:9 doi:10.1016/j.carbpol.2019.115433

83. Shahnaz T, Fazil SMM, Padmanaban VC, Narayanasamy S (2020a) Surface modification of nanocellulose using polypyrrole for the adsorptive removal of Congo red dye and chromium in binary mixture. Int J Biol Macromol 151:322–332. doi:10.1016/j.ijbiomac.2020.02.181
84. Shahnaz T, Sharma V, Subbiah S, Narayanasamy S (2020b) Multivariate optimisation of Cr (VI), Co (III) and Cu (II) adsorption onto nanobentonite incorporated nanocellulose/chitosan aerogel using response surface methodology. J Water Process Eng 36:12. doi:10.1016/j.jwpe.2020.101283
85. Shao et al (2017) Soy protein-based polyethylenimine hydrogel and its high selectivity for copper ion removal in wastewater treatment. JOURNAL OF MATERIALS CHEMISTRY A 5:4163–4171. doi:10.1039/c6ta10814h
86. Sharma PR, Chattopadhyay A, Sharma SK, Geng LH, Hsiao BS (2018a) Nanocellulose from Spinifex as an Effective Adsorbent to Remove Cadmium(II) from Water Acs. Sustainable Chemistry Engineering 6:3279–3290. doi:10.1021/acssuschemeng.7b03473
87. Sharma PR, Chattopadhyay A, Zhan C, Sharma SK, Geng L, Hsiao BS (2018b) Lead removal from water using carboxycellulose nanofibers prepared by nitro-. oxidation method Cellulose 25:1961–1973. doi:10.1007/s10570-018-1659-9
88. Shen C, Zhao YQ, Li WX, Yang Y, Liu RB, Morgen D (2019) Global profile of heavy metals and semimetals adsorption using drinking water treatment residual. Chem Eng J 372:1019–1027. doi:10.1016/j.cej.2019.04.219
89. Silva N, Vilela C, Almeida A, Marrucho IM, Freire CSR (2018) Pullulan-based nanocomposite films for functional food packaging: Exploiting lysozyme nanofibers as antibacterial and antioxidant reinforcing additives. Food Hydrocolloids 77:921–930. doi:10.1016/j.foodhyd.2017.11.039
90. Silva NHCS, Figueira P, Fabre E, Pinto RJB, Freire CSR (2020) Dual nanofibrillar-based bio-sorbent films composed of nanocellulose and lysozyme nanofibrils for mercury removal from spring waters. Carbohyd Polym 238:116210. doi:10.1016/j.carbpol.2020.116210
91. Sirvio JA, Visanko M (2020) Lignin-rich sulfated wood nanofibers as high-performing adsorbents for the removal of lead and copper from water. J Hazard Mater 383:8. doi:10.1016/j.jhazmat.2019.121174
92. Tang C, Brodie P, Brunsting M, Tam KC (2020a) Carboxylated Cellulose Cryogel Beads via a One-step Ester Crosslinking of Maleic Anhydride for Copper Ions. Removal Carbohydrate Polymers 242:116397. doi:10.1016/j.carbpol.2020.116397
93. Tang CX, Brodie P, Li YZ, Grishkewich NJ, Brunsting M, Tam KC (2020b) Shape recoverable and mechanically robust cellulose aerogel beads for efficient removal of copper ions. Chem Eng J 392:11. doi:10.1016/j.cej.2020.124821
94. Tang F et al (2020c) Green acid-free hydrolysis of wasted pomelo peel to produce carboxylated cellulose nanofibers with super absorption/flocculation ability for environmental remediation materials Chem Eng J 395 doi:10.1016/j.cej.2020.125070

95. Tang J, Li X, Bao L, Chen L, Hong FF (2017) Comparison of two types of bioreactors for synthesis of bacterial nanocellulose tubes as potential medical prostheses including artificial blood vessels. Journal of Chemical Technology Biotechnology 92:1218–1228. doi:10.1002/jctb.5111
96. Tong X, Shen WH, Chen XQ, Jia MY, Roux JC (2020) Preparation and mechanism analysis of morphology-controlled cellulose nanocrystals via compound enzymatic hydrolysis of eucalyptus pulp. J Appl Polym Sci 137:11. doi:10.1002/app.48407
97. Uddin MK (2017) A review on the adsorption of heavy metals by clay minerals, with special focus on the past decade. Chem Eng J 308:438–462. doi:10.1016/j.cej.2016.09.029
98. Vadakkekara GJ, Thomas S, Nair CPR (2019) Maleic acid modified cellulose for scavenging lead from water. Int J Biol Macromol 129:293–304. doi:10.1016/j.ijbiomac.2019.02.037
99. Vadakkekara GJ, Thomas S, Nair CPR (2020) Sodium itaconate grafted nanocellulose for facile elimination of lead ion from. water Cellulose 27:3233–3248. doi:10.1007/s10570-020-02983-4
100. Vakili M, Deng S, Cagnetta G, Wang W, Yu G (2019) Regeneration of chitosan-based adsorbents used in heavy metal adsorption. A review Separation Purification Technology 224:373–387. doi:10.1016/j.seppur.2019.05.040
101. Wang C, Yuan Z, Wang A, Qu J, Fang Z, Wen Y (2020a) Ultraviolet light enhanced sodium persulfate oxidation of cellulose to facilitate the preparation of. cellulose nanofibers Cellulose 27:2041–2051. doi:10.1007/s10570-019-02941-9
102. Wang D, Yu H, Fan X, Gu J, Ye S, Yao J, Ni Q (2018a) High Aspect Ratio Carboxylated Cellulose Nanofibers Cross-linked to Robust Aerogels for Superabsorption-Flocculants: Paving Way from Nanoscale to Macroscale. ACS Appl Mater Interfaces 10:20755–20766. doi:10.1021/acsami.8b04211
103. Wang H et al (2015) Facile synthesis of amino-functionalized titanium metal-organic frameworks and their superior visible-light photocatalytic activity for Cr(VI) reduction. J Hazard Mater 286:187–194. doi:10.1016/j.jhazmat.2014.11.039
104. Wang JL, Zhuang ST, Liu Y (2018b) Metal hexacyanoferrates-based adsorbents for cesium removal. Coord Chem Rev 374:430–438. doi:10.1016/j.ccr.2018.07.014
105. Wang Q, Yang L, Jia F, Li Y, Song S (2018c) Removal of Cd (II) from water by using nano-scale molybdenum disulphide sheets as adsorbents. J Mol Liq 263:526–533. doi:10.1016/j.molliq.2018.04.149
106. Wang S et al (2020b) Single molecule observation of hard-soft-acid-base (HSAB) interaction in engineered Mycobacterium smegmatis porin A (MspA). nanopores Chem Sci 11:879–887. doi:10.1039/c9sc05260g
107. Wang ZX, Ji SQ, He F, Cao MY, Peng SQ, Li YX (2018d) One-step transformation of highly hydrophobic membranes into superhydrophilic and underwater superoleophobic ones for high-efficiency separation of oil-in-water emulsions. Journal of Materials Chemistry A 6:3391–3396. doi:10.1039/c7ta10524j

108. Xu QH, Wang YL, Jin LQ, Wang Y, Qin MH (2017) Adsorption of Cu (II), Pb (II) and Cr (VI) from aqueous solutions using black wattle tannin-immobilized nanocellulose. J Hazard Mater 339:91–99. doi:10.1016/j.jhazmat.2017.06.005
109. Yang R, Aubrecht KB, Ma HY, Wang R, Grubbs RB, Hsiao BS, Chu B (2014) Thiol-modified cellulose nanofibrous composite membranes for chromium (VI) and lead (II). adsorption Polymer 55:1167–1176. doi:10.1016/j.polymer.2014.01.043
110. Yani J, Jiping Z, Qi Z, Guoqi Z, Xiaodong X (2017) Comparative analysis of nanocellulose from Humulus scandens stems using four isolation methods Pratacultural ence
111. Yantasee W et al (2007) Removal of Heavy Metals from Aqueous Systems with Thiol Functionalized Superparamagnetic Nanoparticles Environmental science &. technolog 41:5114–5119
112. Yao C, Wang F, Cai Z, Wang X (2016) Aldehyde-functionalized porous nanocellulose for effective removal of heavy metal ions from aqueous solutions. Rsc Advances 6:92648–92654. doi:10.1039/c6ra20598d
113. Yu H, Hong HJ, Kim SM, Ko HC, Jeong HS (2020) Mechanically enhanced graphene oxide/carboxymethyl cellulose nanofibril composite fiber as a scalable adsorbent for heavy metal removal Carbohydrate Polymers 240 doi:10.1016/j.carbpol.2020.116348
114. Yu X, Tong S, Ge M, Wu L, Zuo J, Cao C, Song WJ (2013) Adsorption of heavy metal ions from aqueous solution by carboxylated cellulose nanocrystals. J Environ Sci 000:P.933–P943
115. Zhang N, Zang G-L, Shi C, Yu H-Q, Sheng G-P (2016) A novel TEMPO-mediated oxidized cellulose nanofibrils modified with PEI: Preparation, characterization, and application for Cu(II) removal. J Hazard Mater 316:11–18. doi:10.1016/j.jhazmat.2016.05.018
116. Zhang X, Elsayed I, Navarathna C, Schueneman GT, Materials EBHJAA, Interfaces (2019) Biohybrid Hydrogel and Aerogel from Self-Assembled Nanocellulose and Nanochitin as a High-Efficiency Adsorbent for Water Purification. ACS Applied Materials 11:46714–46725. doi:10.1021/acsami.9b15139
117. Zhao JQ, Zhang XF, He X, Xiao MJ, Zhang W, Lu CH (2015) A super biosorbent from dendrimer poly(amidoamine)-grafted cellulose nanofibril aerogels for effective removal of Cr(VI). Journal of Materials Chemistry A 3:14703–14711. doi:10.1039/c5ta03089g
118. Zheng QF, Cai ZY, Gong SQ (2014) Green synthesis of polyvinyl alcohol (PVA)-cellulose nanofibril (CNF) hybrid aerogels and their use as superabsorbents. Journal of Materials Chemistry A 2:3110–3118. doi:10.1039/c3ta14642a
119. Zhou M, Guo J, Yang C (2018) Ratiometric fluorescence sensor for Fe~(3+) ions detection based on quantum dot-doped hydrogel optical fiber. Sensors Actuators B: Chemical B 264:52–58
120. Zhou Y, Fu S, Zhang L, Zhan H, Levit MV (2013) Use of carboxylated cellulose nanofibrils-filled magnetic chitosan hydrogel beads as adsorbents for Pb(II). Carbohyd Polym 101:75–82. doi:10.1016/j.carbpol.2013.08.055
121. Zhu H et al (2011) Biosynthesis of spherical Fe3O4/bacterial cellulose nanocomposites as adsorbents for heavy metal ions. Carbohyd Polym 86:1558–1564.

doi:10.1016/j.carbpol.2011.06.061

# Figures

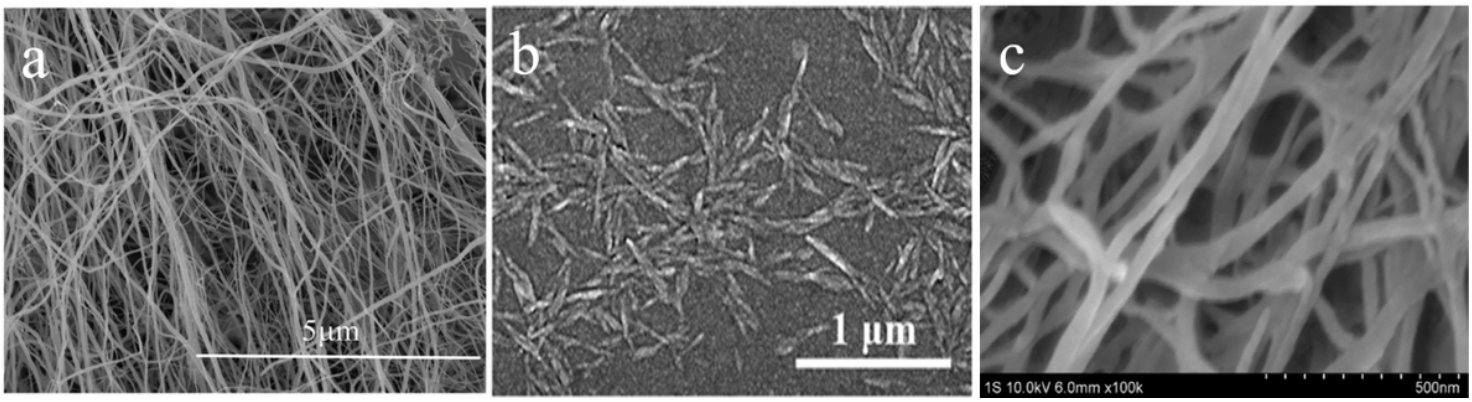


**Figure 1**

(a) SEM images of NFCs(Wang et al. 2020a).(b) CNCs(Li et al. 2019b).(c) BNCs(Zhu et al. 2011)

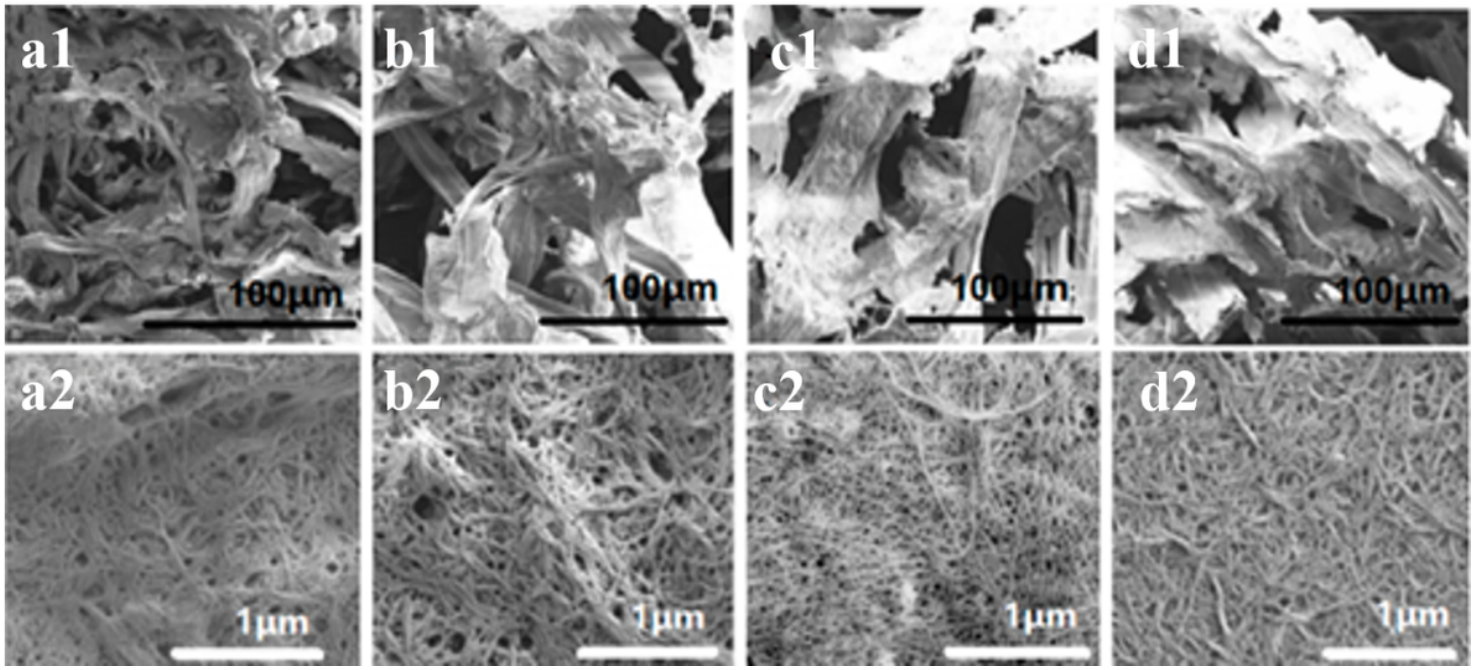


**Figure 2**

(a1, a2) FE-SEM images of aerogels pore structure and high magnification for S-CNF, (b1, b2) 9-CNF, (c1, c2) 7-CNF, (d1, d2) 5-CNF(Wang et al. 2018a)

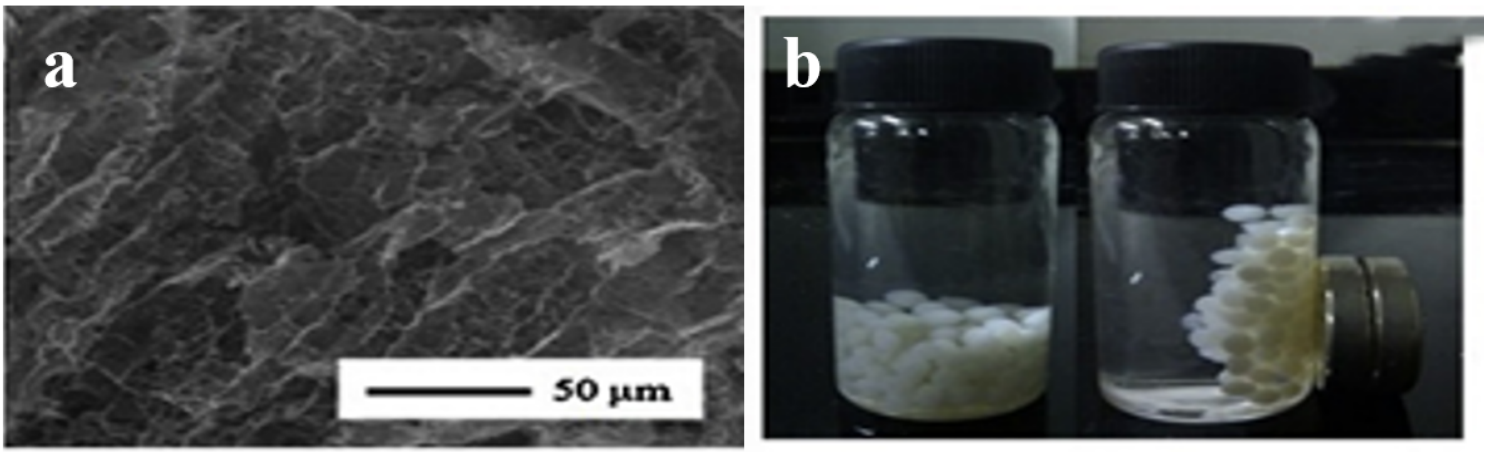


Figure 3

(a) SEM image of m-cs/PVA/CCNFs hydrogel. (b) photographs of m-cs/PVA/CCNFs hydrogel in Pb2+ solution before and after magnetic separation by an external magnetic field.

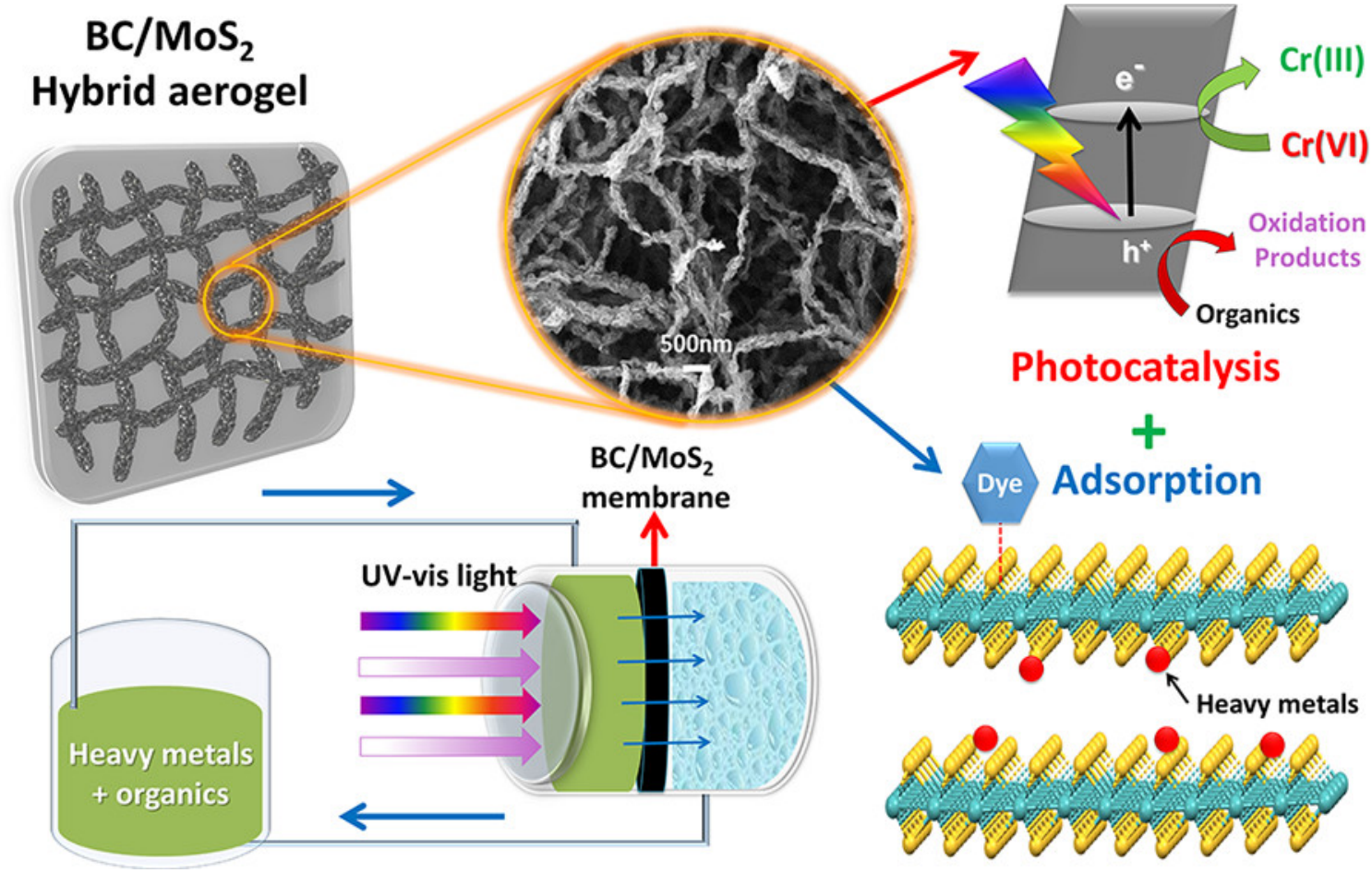


Figure 4

Removal mechanism of heavy metal ions in BC/MoS2 hybrid aerogel (Ferreira-Neto et al. 2020)

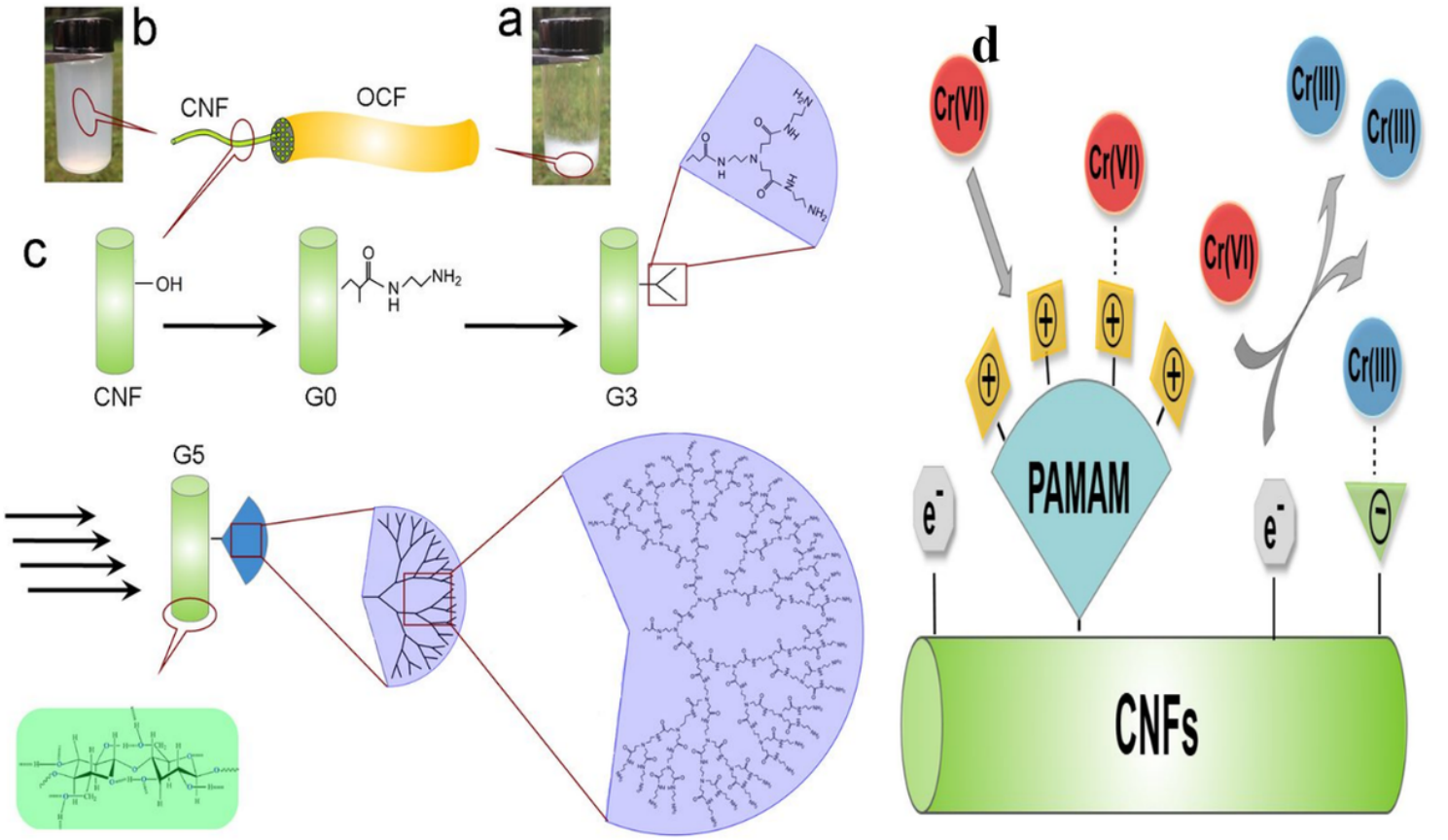


**Figure 5**

(a) 0.1wt%dispersions of original cellulose fibers. (b CNFs after being left to stand for 3 days. (c) The preparation method of PAMAM-g-CNFs. (d The mechanism of PAMAM-g-CNFs to remove Cr6+ in water(Zhao et al. 2015)

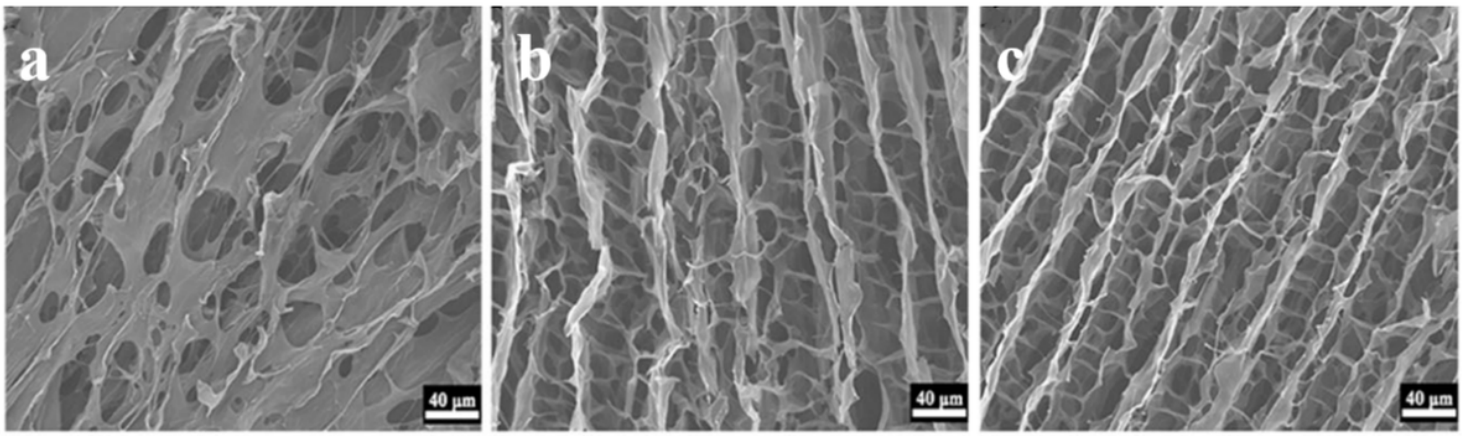


**Figure 6**

(a)SEM images of CNF, (b) CNF–1MPTMS, (c) CNF–2MPTMS sponges(Rong et al. 2018)

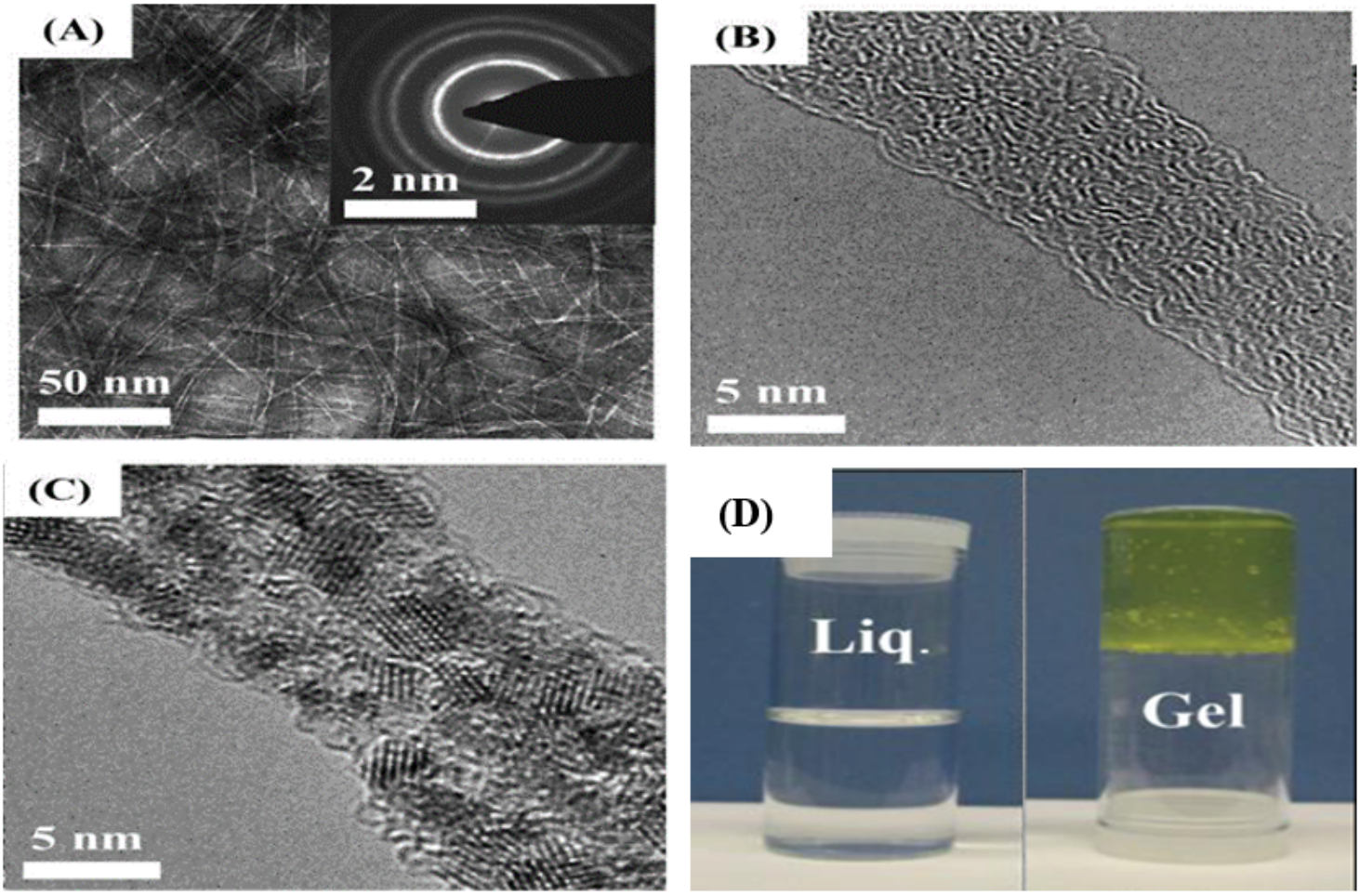


## Figure 7

(A) TEM image of the corresponding electron diffraction pattern of cellulose nanofibers; (B) high resolution TEM image of a cellulose nanofiber before the adsorption of UO22+; (C) high resolution TEM image of a cellulose nanofiber after the adsorption of UO22+(D) After adsorption of UO22+, cellulose nanofiber Liq. was transformed into Gel (Ma et al. 2013)

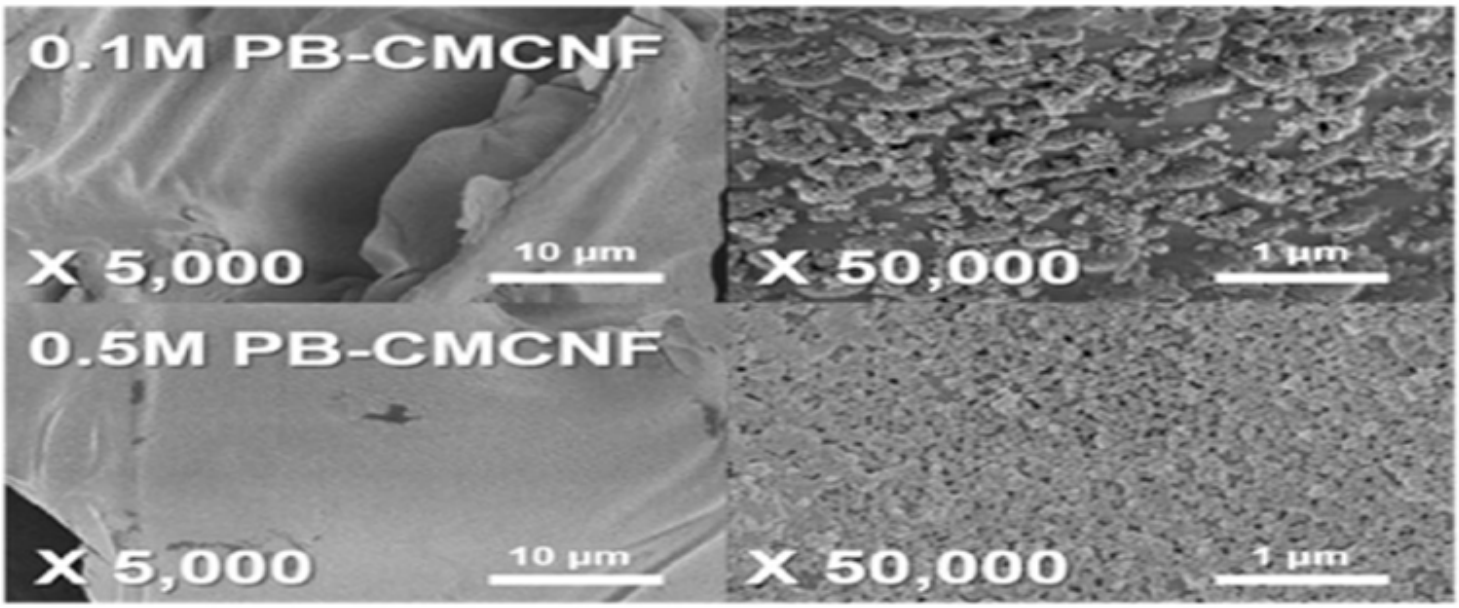


**Figure 8**

SEM images of PB-CMCNF membranes(Eun et al. 2020)

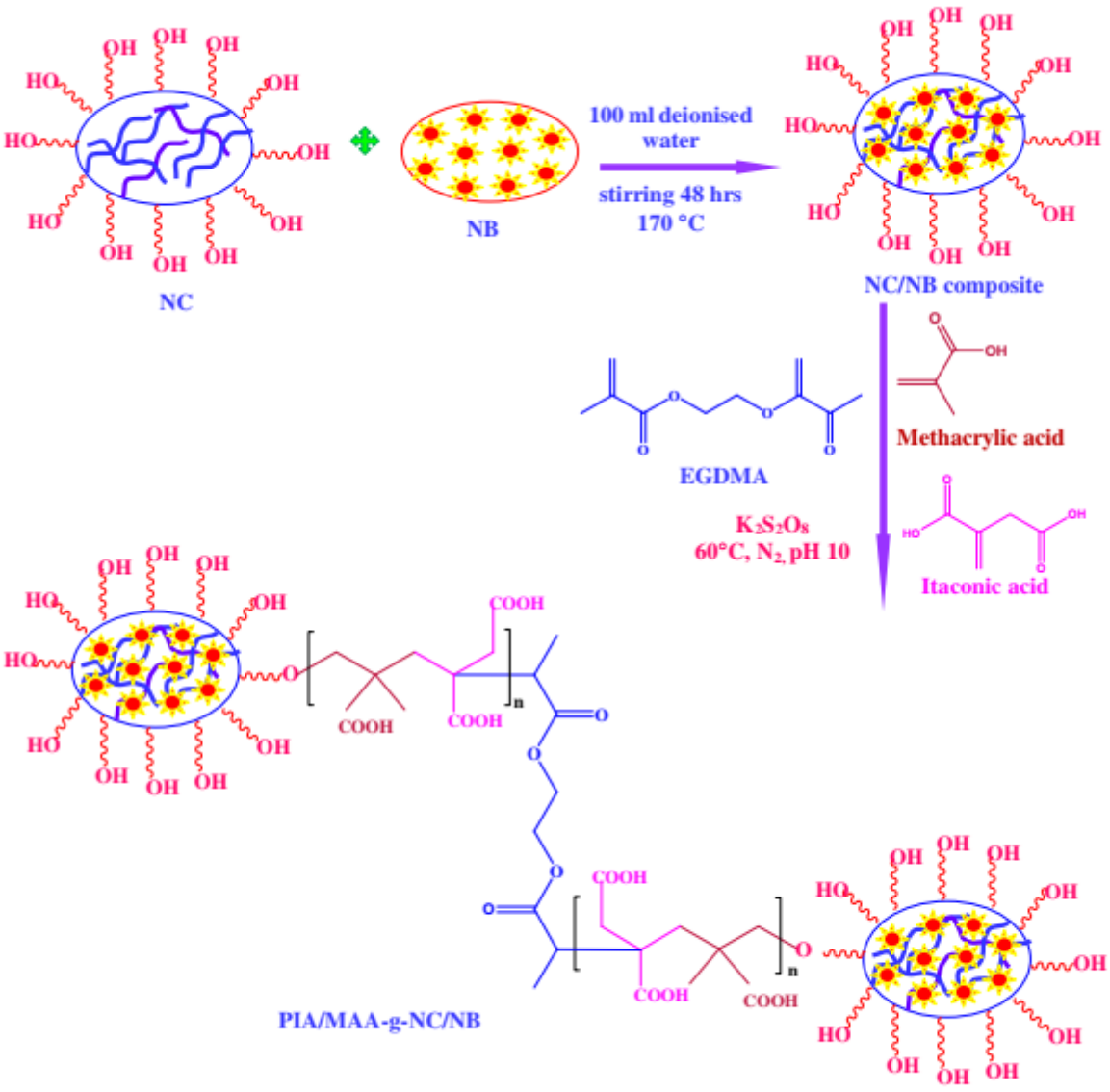


## Figure 9

Synthesis of P(IA/MAA)-g-NC/NB (Anirudhan et al. 2015)

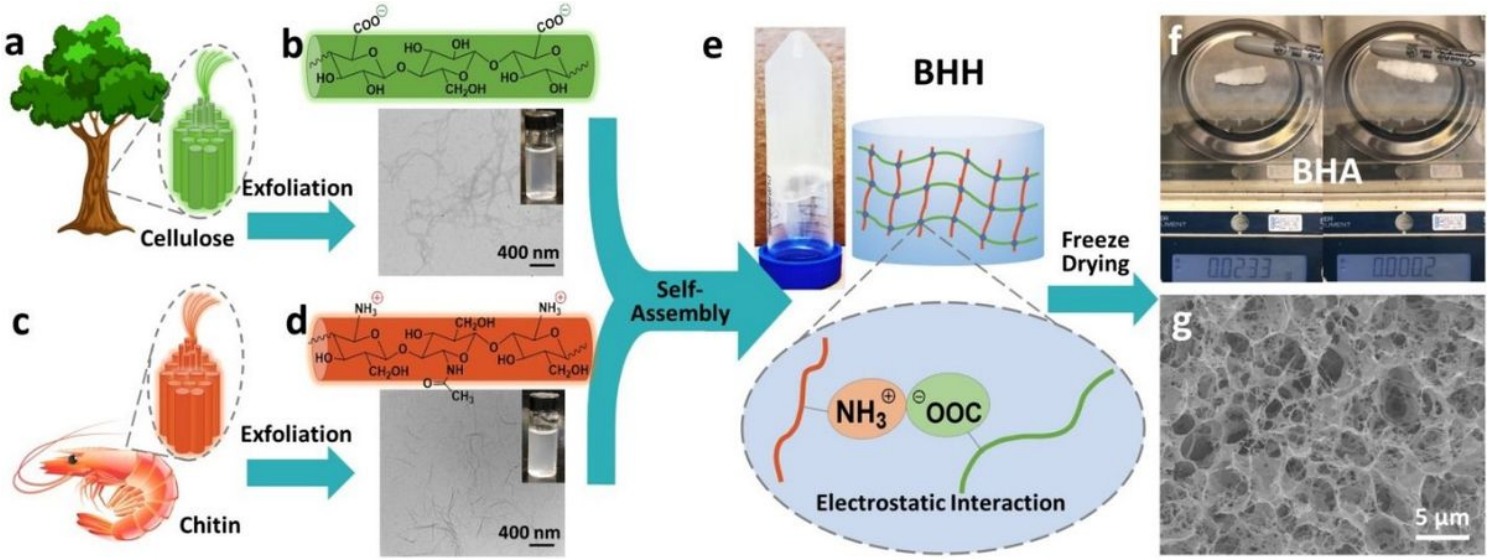

## Figure 10

Schematic of the self-assembly process for the production of BHH and BHA. (a-b) TEMPO- and mechanical-exfoliation to produce TOCNF; (c-d) NaOH- and mechanical-exfoliation to produce PDChNF; (e) electrostatic force induced self-assembly gelation of nanofibers with ionic interactions between TOCNF and PDChNF; (f) digital images illustrate the ultra-light BHA was captured by a marker pen due to static electricity; (g) scanning electron microscopy (SEM) image of BHA exhibits a highly porous structure(Zhang et al. 2019).

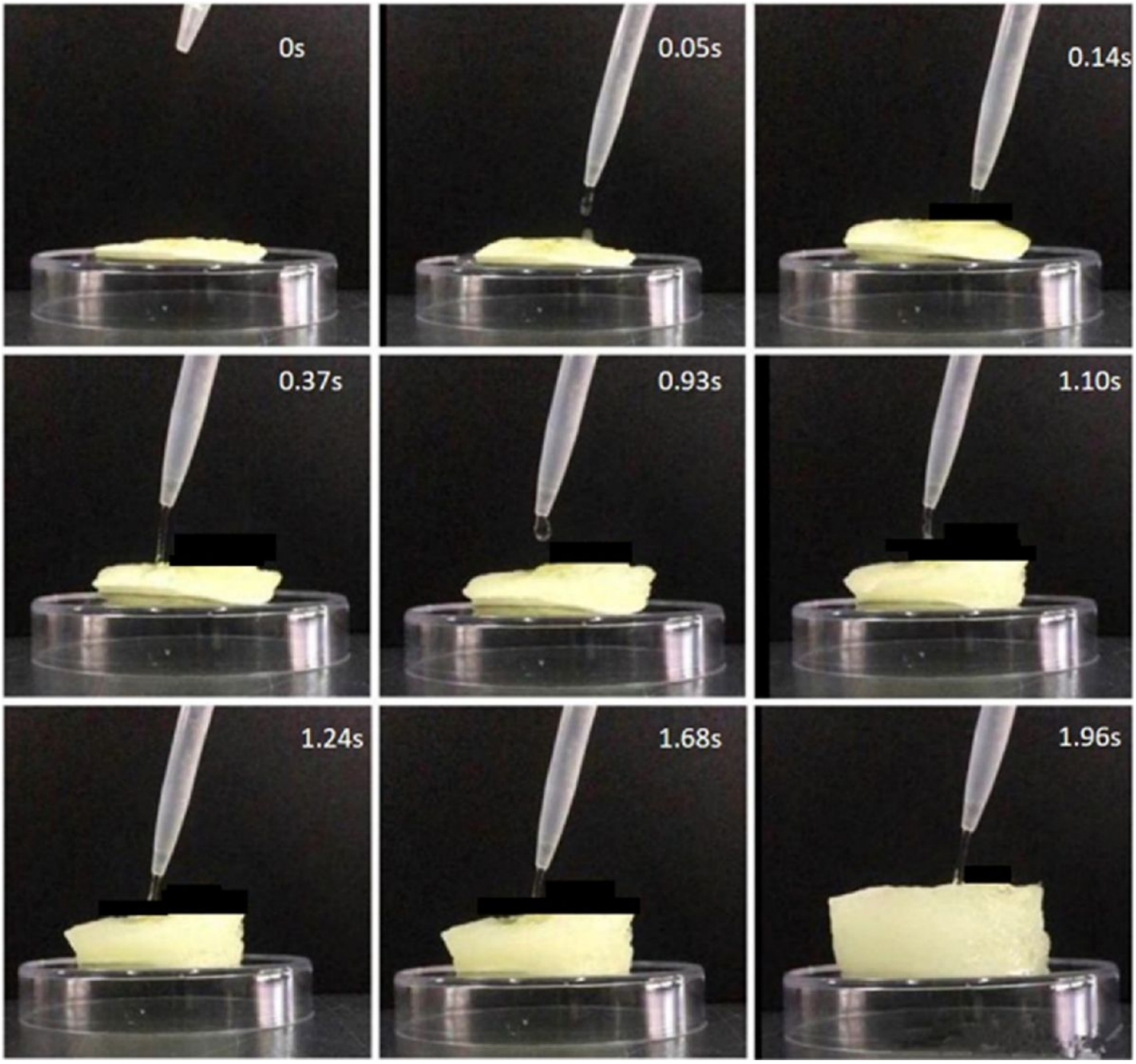


## Figure 11

Shape recovery of NPA22 by absorbing water(Li et al. 2018a)

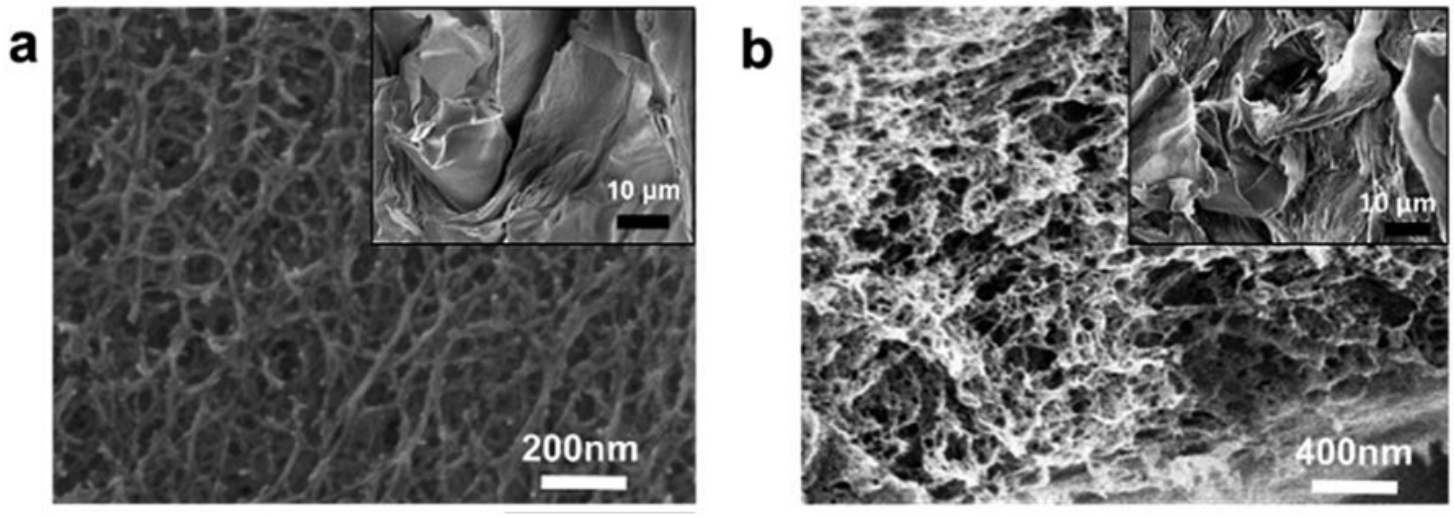


**Figure 12**

(a)SEM images of as-prepared CNFs. (b)DACs(Yao et al. 2016).

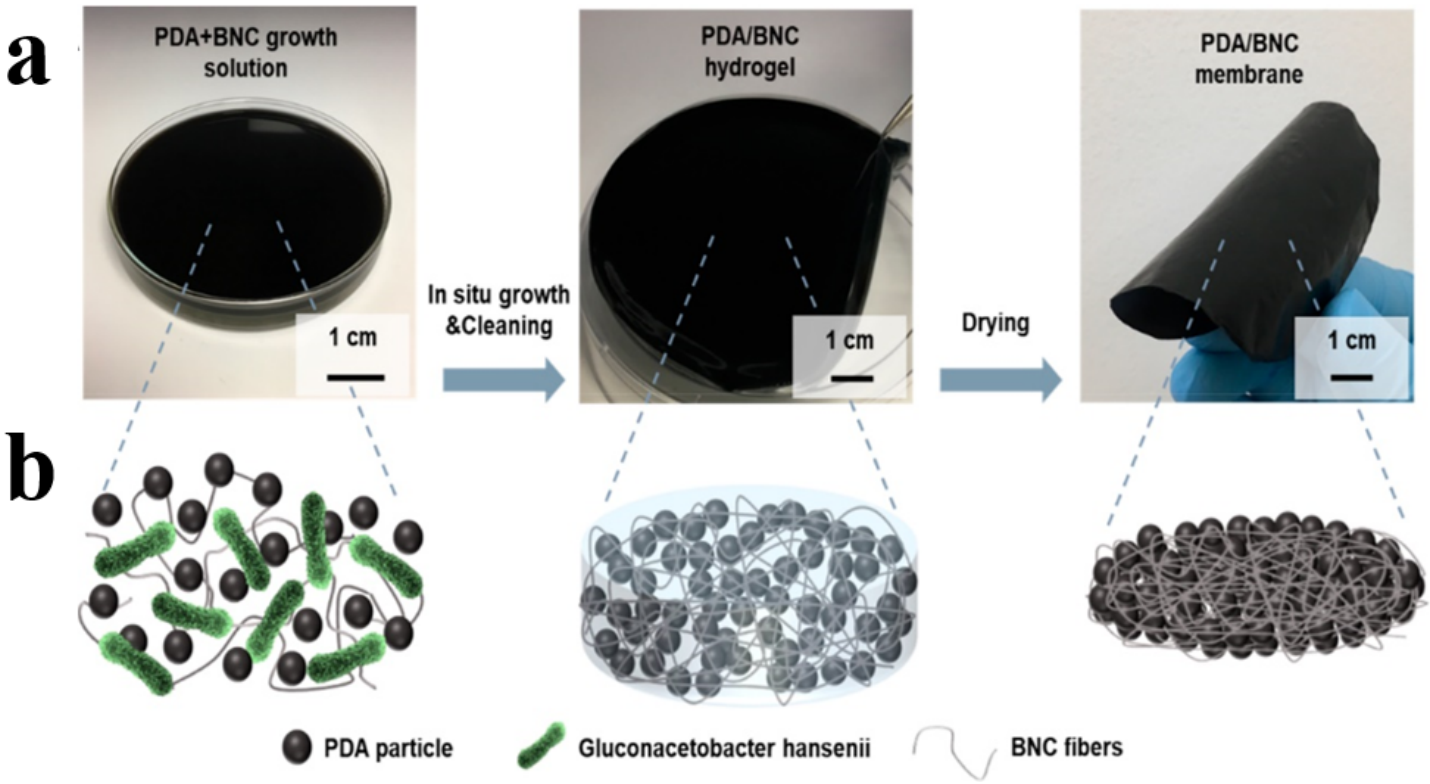


**Figure 13**

(a)Photographs of PDA/BNC membrane during different fabrication steps. (b) Schematic representation of the fabrication process of PDA/BNC membrane(Derami et al. 2019).

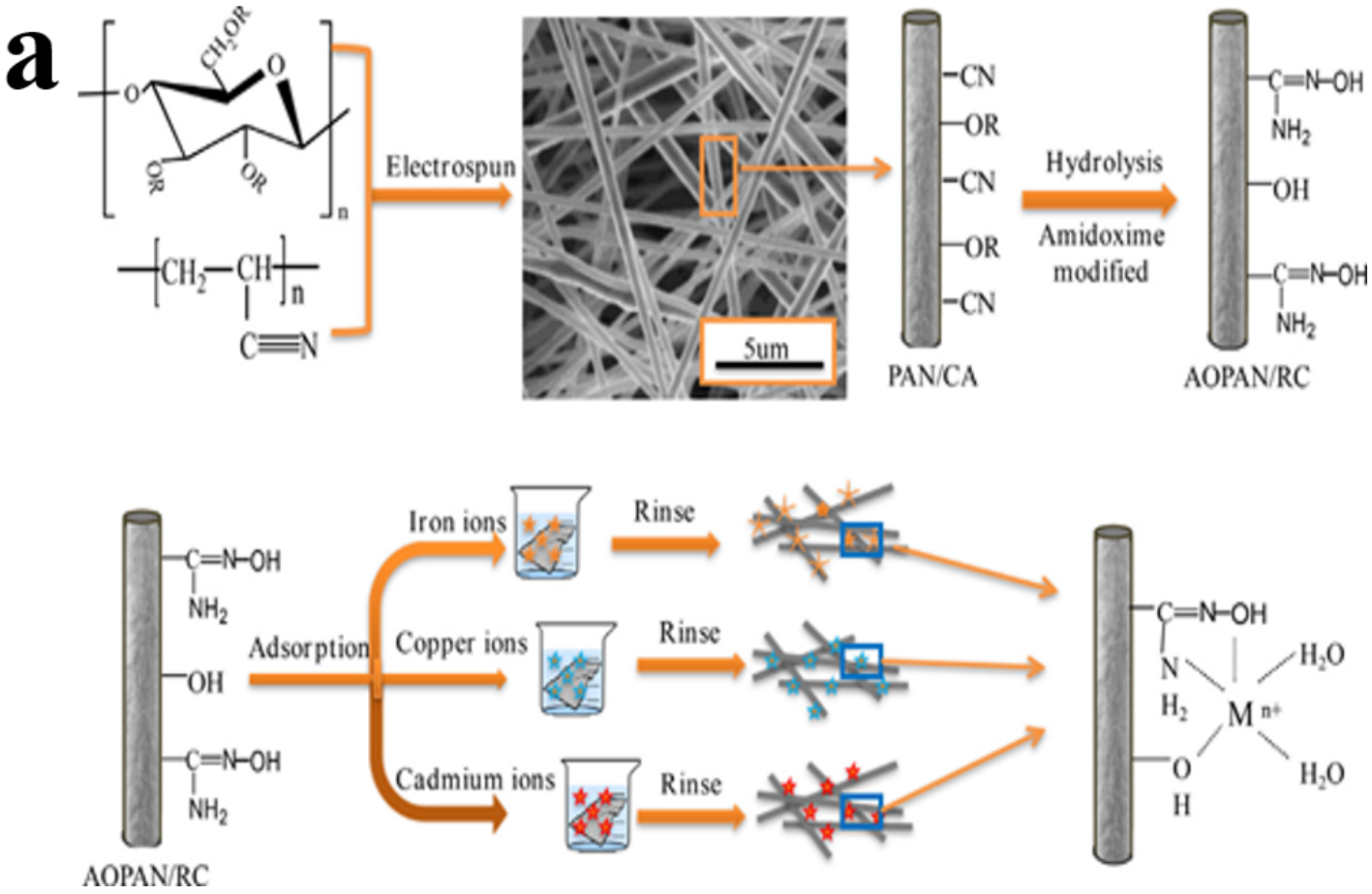


**Figure 14**

Schematic illustration showing the preparation and evaluation of electrospun AOPAN/RC blend nanofiber membrane for adsorption/removal of heavy metal ions from water(Feng et al. 2018).

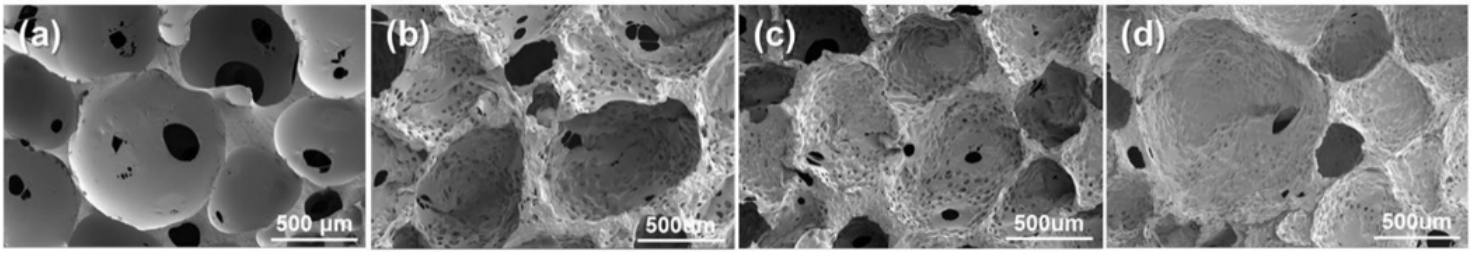


**Figure 15**

(a)Surface SEM images of neat PU foam (b)PU/CMCNF composite foams of 2 wt%. (c) 3 wt%. (d) 4 wt% CMCNF. (Hong et al. 2018).

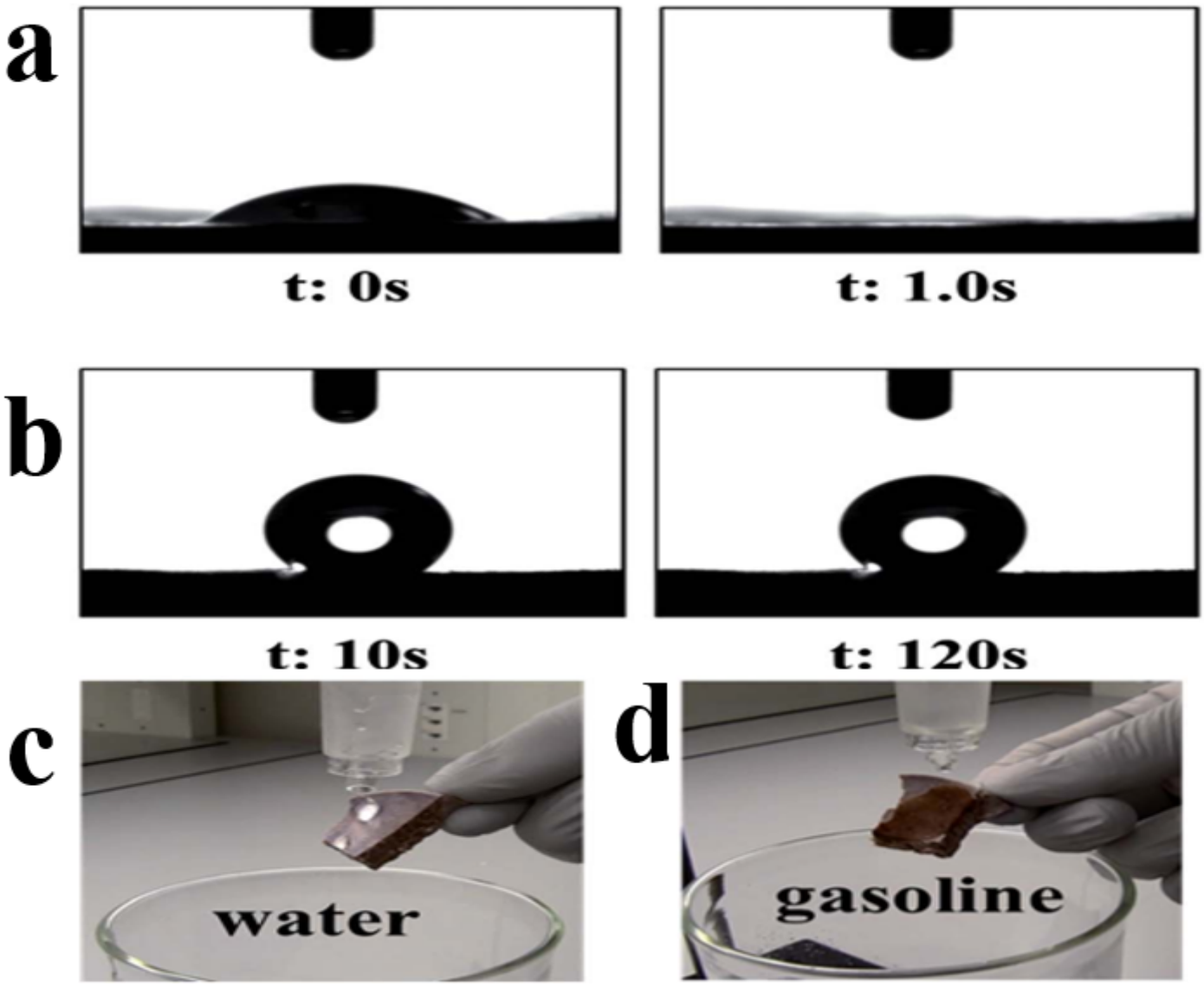


## Figure 16

Water contact angle measurements of the PVA/CNF aerogels:(a) uncoated aerogel and (b) silane-coated aerogel. Optical images of (c) water droplets and (d) gasoline droplets squirted on a piece of silane-coated PVA/CNF aerogel (Zheng et al. 2014)

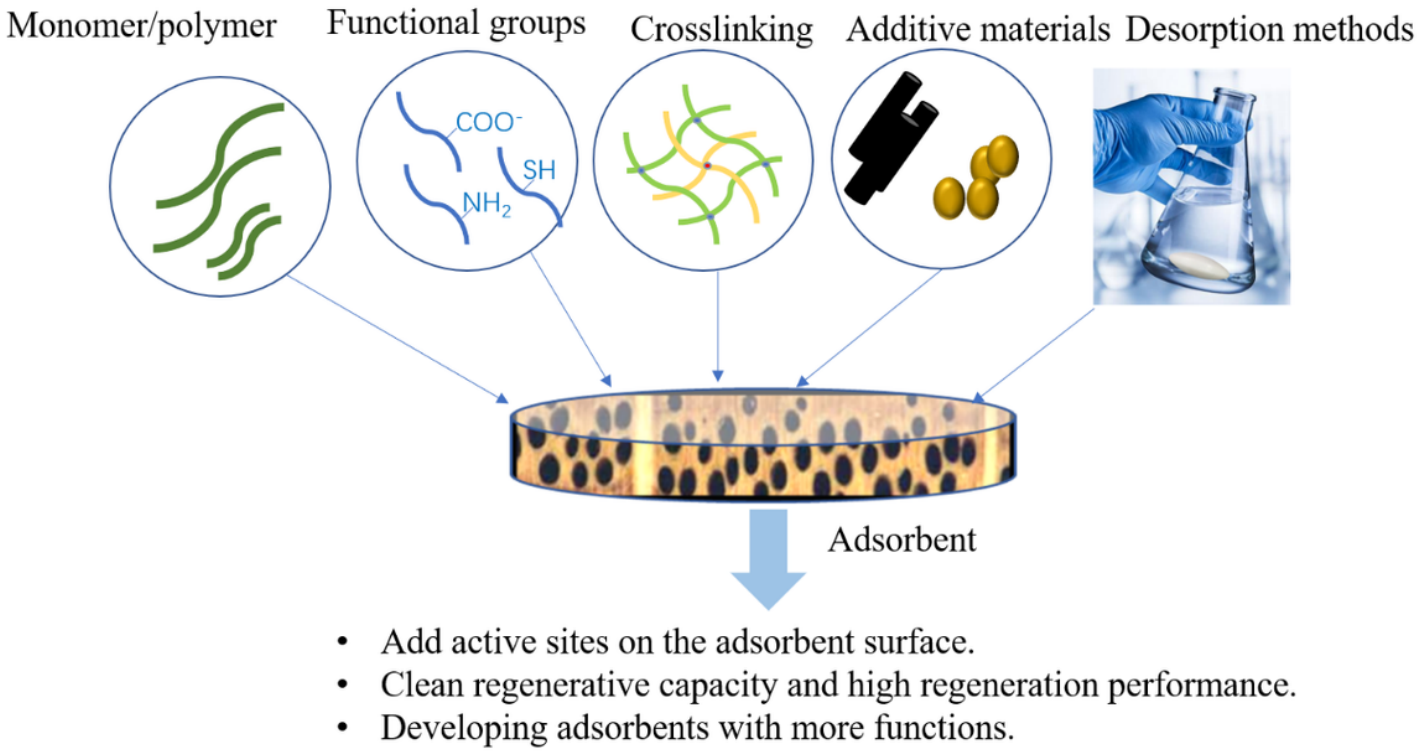


**Figure 17**

By regulating key elements including monomers/polymers with different functional groups, cross-linking types, desorption methods endorse nanocellulose based adsorbents with many advanced properties to excel in heavy ions removal applications.

## Supplementary Files

This is a list of supplementary files associated with this preprint. Click to download.

- graphicalabstract.png